LA-UR-19-22478
Approved for public release; distribution is unlimited.

Title: Modeling aqueous and non-aqueous electrolyte solutions from first principle approaches

Author(s): Karmakar, Anwesa

Intended for: Report

Issued: 2019-03-18

Modeling aqueous and non-aqueous electrolyte solutions from first principle approaches

Anwesa Karmakar

IIT Kanpur, India

LANL, USA

Modeling aqueous electrolyte solutions from first principle approaches

Anwesa Karmakar

IIT Kanpur, India

Funding Resources

Department of Science & Technology, Government of India

सत्यमेव जयते

LANL, USA

A. Karmakar et al., Chem. Phys, 412, 13-21 (2013)

A. Karmakar and A. Chandra, Chem. Phys, 418, 1-8 (2015)

A. Karmakar and A. Chandra, J. Phys. Chem. B, 119, 8561-8572 (2015)

A. Karmakar and A. Chandra, J. Chem. Phys. 2015, 142 (16), 1654505-10

A. Karmakar, J. Mol. Liq., 279, 306-316 (2019)

A. Karmakar, J. Comp. Chem., Under Review, 2019

Introduction

- Structure and Dynamical properties of water plays a vital role in many chemical and biological processes

- Strong coupling between water and ion results well defined structures that alters the dynamics of water.

- Hofmeister series effects: Effect of ion on protein stability and solubility

  - The role of dispersion forces
  - How do the ions effect the dynamics of the systems

"Recent theoretical study has confirmed that the solvation energy between the ion and surrounding water molecules underlies the mechanisms of Hofmeister series"

- The random motion of water molecules produces vibrational spectral diffusion in presence of the surrounding environment.

- Water at supercritical temperature is known as environmentally benign solvent medium.

Hofmeister series of cations

$$NH_4^+ > K^+ > Na^+ > Li^+ > Mg^{2+} > Ca^{2+} > \text{guanidinium}$$

Hofmeister series of anions

$$F^- \approx SO_4^{2-} > HPO_4^{2-} > \text{acetate} > Cl^- > NO_3^- > Br^- > ClO_3^- > I^- > ClO_4^- > SCN^-$$

Adreev et al. 2017, 2018, J. Phys. Chem. B

Experimental Findings

- X-ray and Neutron Scattering
  - Structural informations
- Low frequency Raman (<200 cm^{-1})
  - Intermolecular (low frequency) and Intramolecular (high frequency) motion
- Transient hole burning IR laser experiments
  - Rotational and Hydrogen bond dynamics

D. H. Powell *et al*. *Faraday Discuss. Chem. Soc.* **1988**, *85*, 137.; J. E. Enderby *Chem. Soc. Rev.* **1995**, *24*, 159.; N. Skipper *et al J. Phys.: Condens. Matter* **1989**, *1*, 4141. J. -J. Max *et al. J. Chem. Phys.* **2001**, *115*, 2664; Y. Wang *et al. J. Chem. Phys.* **1994**, *101*, 3453.; K. Mizoguchi *et al. ibid* **1998**, *109*, 1867.; Y. Amo *et al. Phys. Rev. E* **1998**, *58*, 7553.; Soper *et al Chem Phys* **2000**, 258; P. Hamm *et al. Phys. Rev. Lett.* **1998**, *81*, 5326.

Methodology

Car Parrinello Molecular Dynamics and CPMD code to generate the time dependent trajectories

Wavelet analysis for frequency calculation

1. Vibrational spectral diffusion

    1. Frequency-frequency time correlation
    2. Hole Burning technique

2. Population correlation approach

    1. Hydrogen bond dynamics
    2. Orientational relaxation
    3. Residence dynamics
    4. Dielectric Relaxation (electric field fluctuation)
    5. Power spectra : velocity-velocity auto correlation function approach

3. Diffusion

R. Car and M. Parrinello, *Phys. Rev. Lett.* **55**, 2471 (1985), CPMD CODE;D. Marx, J. Hutter, Ab Initio Molecular Dynamics: Basic Theory and Advanced Methods, Cambridge University Press, Cambridge, 2009.

L. V. Vela-Arevalo and S. Wiggins, *Int. J. Bifur. Chaos* **11**, 1359 (2001), *Statistical Methods for Spatio-Temporal Systems*, Chapter-3, edited by B. Finkenstädt, L. Held and V. Isham, Chapman & Hall/CRC, Boca Raton (2007).

*R. Rey, K. B. Moller, and J. T. Hynes, *J. Phys. Chem. A*, **106** 11993(2002); K. B. Moller, R. Rey, and J. T. Hynes, *J. Phys. Chem. A*, **108** 1275(2004).

A. Karmakar et al. Chem. Phys. 2013, JPCB, 2015, JCP, 2015, Chem. Phys. 2015, J. Mol. Liq. 2019, J. Comp. Chem. Under Review, 2019

Experimental Findings Aqueous Bromide and Iodide ion Solutions

- The aqueous solutions (Cl^-, Br^-, I^-) show vibrational spectral diffusion of multiple time scales through several decay channels.
- Stochastic modulation time(τ_c):3-4 ps, in addition to a shorter time scale of less than a ps.
- The spectral diffusion was found to increase from 2.6 to 4.8 ps with increasing concentration of aqueous bromide ion solution.

H. J. Bakker *et al. Chem. Rev.* **2010**; *J. Phys. Chem. A* **2009**, *113*, 6104.

S. Park *et al. Proc. Natt. Acad. Sci; U.S.A* **2007**, *104*, 16731.

Aqueous Azide ion Solution

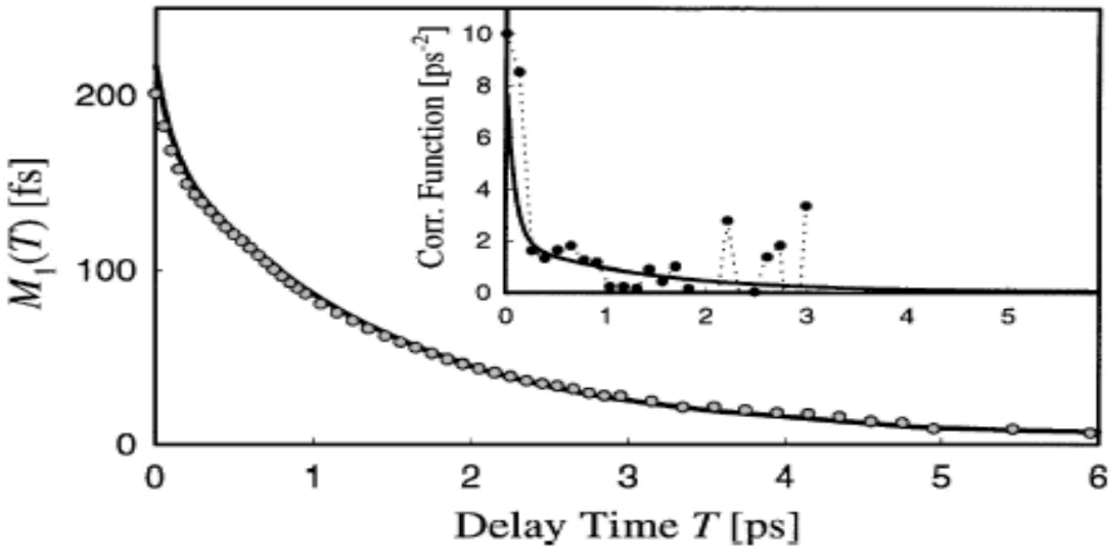

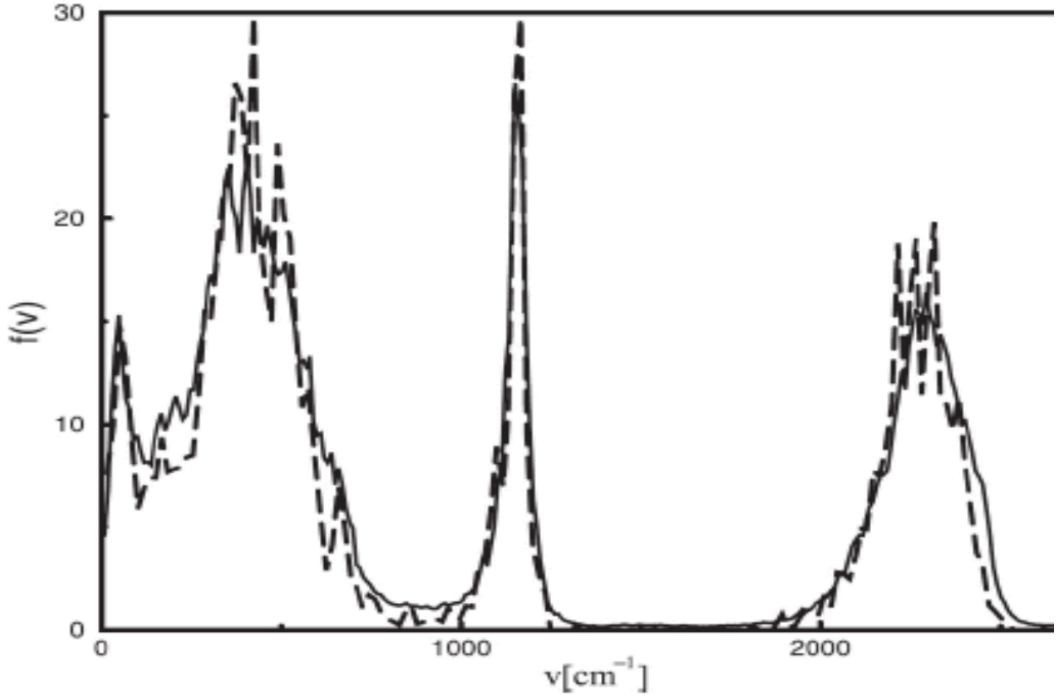

- τ_{short} ~ 80 fs and τ_{long} ~ 2.4 ps in D_2O.

- Orientational relaxation of azide molecule in D_2O occurs at 7.1 ps.
  Solvent induced stabilization of valence bond resonance structures of azide molecular ion $N{\equiv}N^{+}\text{-}N^{2-} \leftrightarrow N^{-}{=}N^{+}{=}N^{-} \leftrightarrow N^{-2}\text{-}N^{+}{\equiv}N$

D. Yarne *et al. Chemical Physics* **2000**, *258*, 163.; Hamm *et al. Phys. Rev. Lett.* **1998**, *81*, 5326.; J.C.Owrutsky *et al. Chem. Phys. Lett.* **1991**, *184*, 368.; M. Ferrario *et al. Chem. Phys. Lett.* **1993**, *213*, 537.

Aqueous Bromide ion Solutions

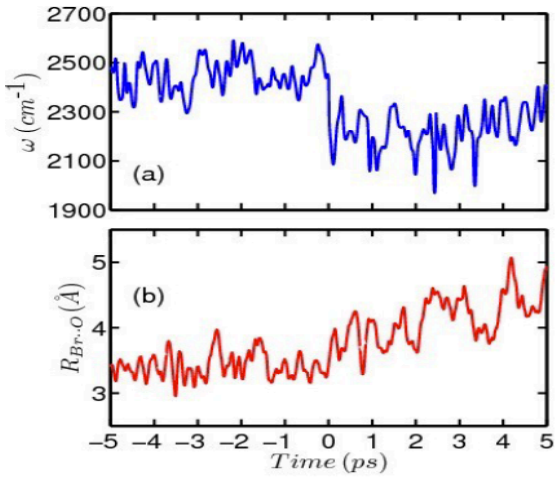

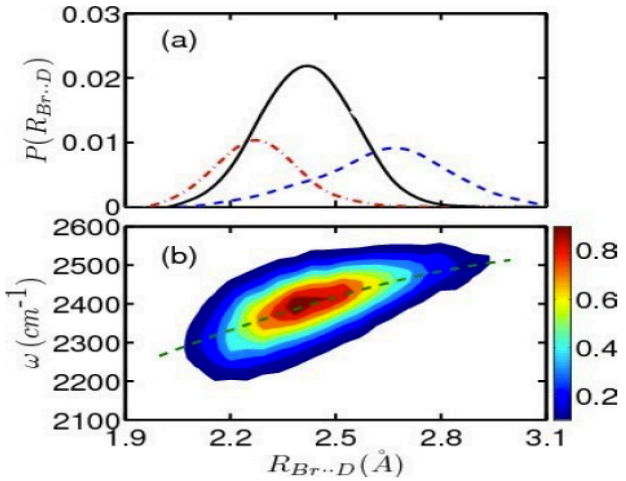

- Average frequencies cm^{-1} : 2400 (inside solvation shell), 2370 (bulk)
- No change is observed in OD stretching frequency in solvation shell and in bulk at conc. soln.
- Joint probability distribution of observing a particular frequency for a given hydrogen bond (Br···D) length.

Spectral diffusion: $f(t) = a_0 \cos(\omega_S t)e^{-\frac{t}{\tau_0}} + a_1 e^{-\frac{t}{\tau_1}} + (1 - a_0 - a_1)e^{-\frac{t}{\tau_2}}$

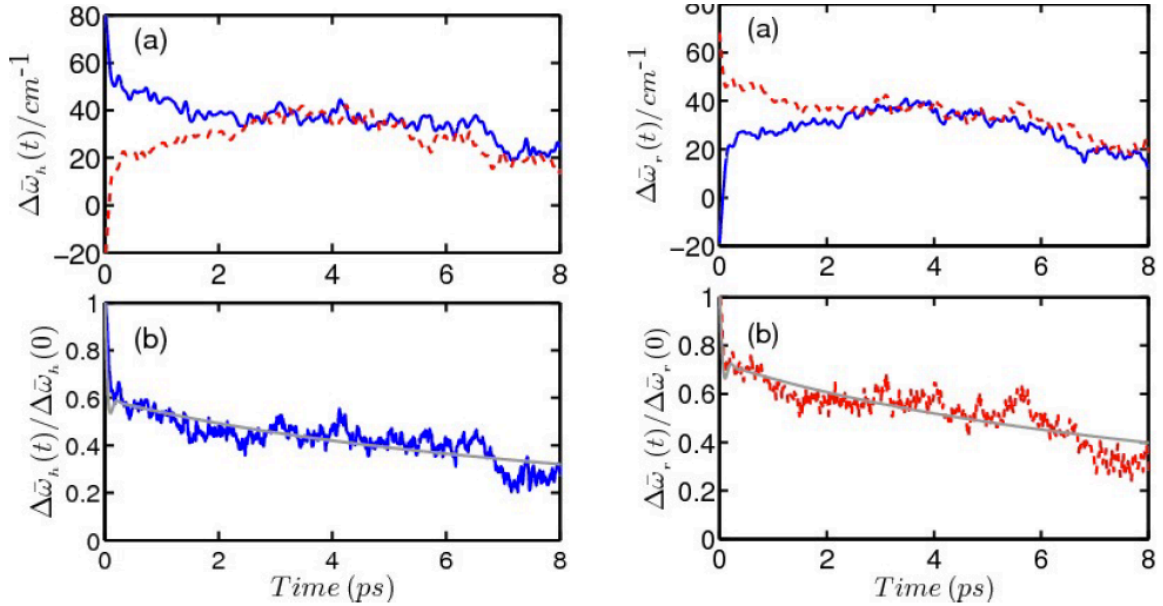

The average lifetimes of bromide ion–water and all hydrogen bonds (HBs) of the dilute (System 1) and concentrated (System 2) solutions for all functionals. Results are also included for the residence times of water in the ion hydration shell. All time constants are expressed in ps. The values shown in brackets are for the BLYP functional [34].

Quantity	System	Ion–water HBs	All HBs
τ_{HB}	1	0.94(1.75)	1.90(3.20)
τ_R	1	9.98(18.0)	–
τ_{HB}	2	1.21(2.20)	1.54(2.50)
τ_R	2	16.56(20.3)	–

Functional	Quantity	Excitation	τ_0(ps)	τ_1(ps)	τ_2(ps)	$\omega_s(cm^{-1})$ a_0	a_1
BLYP	$\Delta\bar{\omega}_h(t)$	Blue	0.10	3.52	19.32	127.4	0.40	0.13
BLYP-D	$\Delta\bar{\omega}_h(t)$	Blue	0.23	1.67	8.52	93.52	0.16	0.48
BLYP	$\Delta\bar{\omega}_r(t)$	Red	0.072	3.12	18.0	132.5	0.27	0.12

- **The ion water hydrogen bond dynamics is faster with respect to the water-water HB dynamics.**
- **The residence time of the ion in the solvation shell of the is noticeable: Ions appears as an structure breaker in this case (Chaotropic Properties).**
- **Dispersion interaction produces faster dynamics.**

A. Karmakar et al., Chem. Phys, 412, 13-21 (2013)

A. Karmakar and A. Chandra, Chem. Phys, 418, 1-8 (2015)

Aqueous Iodide ion Solutions

Table 1. Average Lifetimes of Iodide Ion—Water and All Hydrogen Bonds (HBs) of the Dilute and Concentrated Solutions[a]

quantity	system	functional	ion—water HBs	all HBs
τ_{HB}	1	BLYP	1.00	2.43
τ_R	1	BLYP	12.62	—
τ_{HB}	2	BLYP	1.31	1.61
τ_R	2	BLYP	16.42	—
τ_{HB}	3	BLYP-D	0.67	1.81
τ_R	3	BLYP-D	16.40	—
τ_{HB}	4	BLYP-D	0.80	1.28
τ_R	4	BLYP-D	19.20	—

[a]Results are also included for the residence times of water in iodide ion hydration shells. All time constants are expressed in picoseconds.

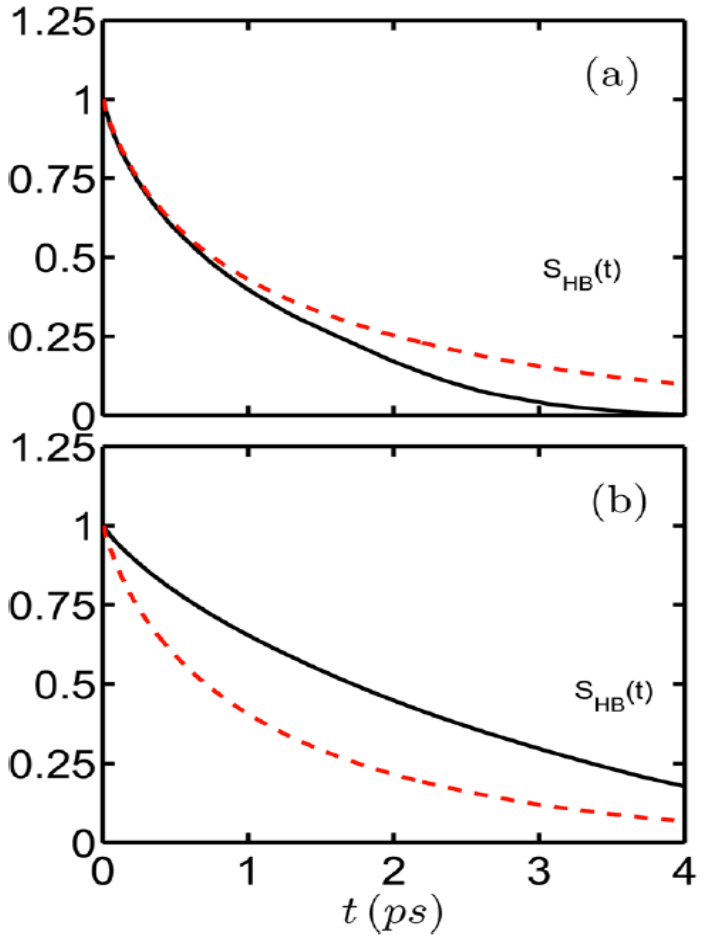

Figure 5. Time dependence of the continuous hydrogen bond correlation function ($S_{HB}(t)$) of systems 1 (solid) and 2 (dashed). The results of part a are for only I^-—water hydrogen bonds and those of part b are for all the hydrogen bonds present in systems 1 and 2. These figures are for the BLYP functional.

- **I^- --- water HB bond is weaker w.r.t the water-water HB bond.**
- **The hydrogen bond lifetime is found to be slower w.r.t the dilute soln.**
- **Effect of concentration on the HB lifetime and dynamics is clear.**

A. Karmakar and A. Chandra, J. Phys. Chem. B, 119, 8561-8572 (2015)

Supercritical Aqueous Bromide and Iodide ion Solutions

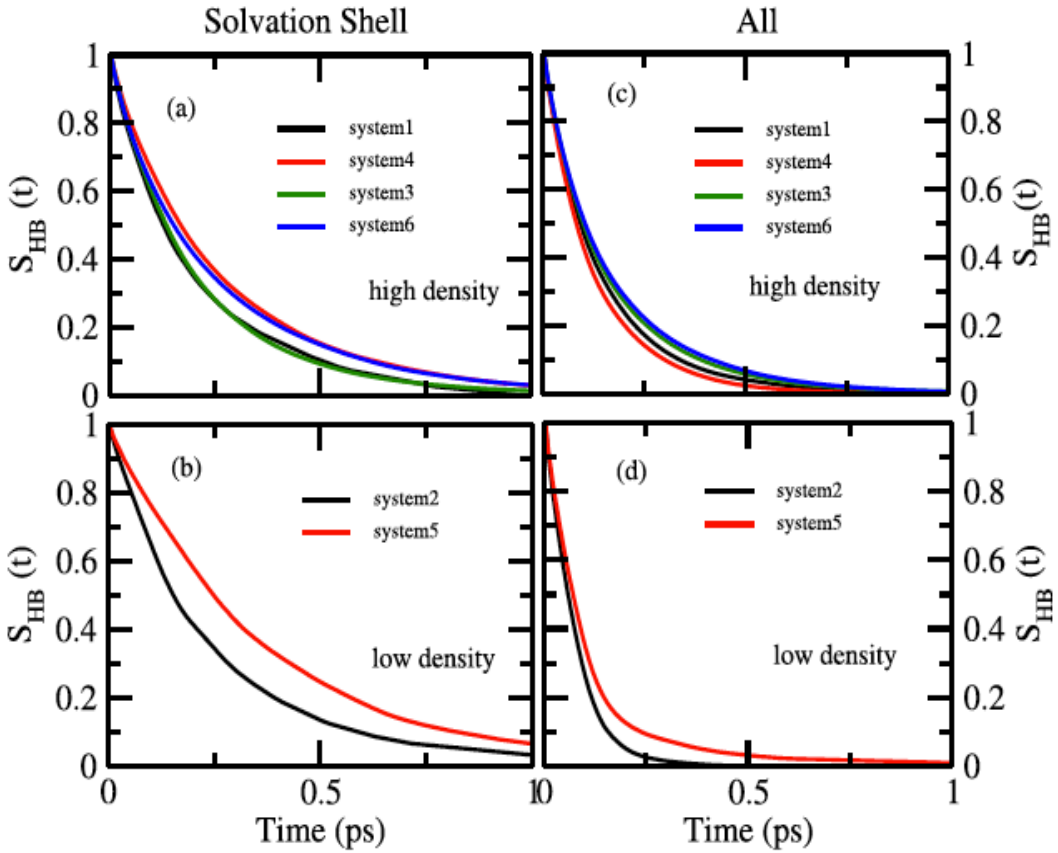

Table 3
The average lifetimes of hydrogen bonds, residence times and dangling bond of water molecules in anion hydration shells and for all modes. All time scales are expressed in ps. Mass density has been used for heavy water (for convenience).

Quantity	Systems	Mass density ($g\,cm^{-3}$)	Solvation shell modes	All modes
τ_{HB}	Aq. Br^-	1.18 (1)	0.20	0.15
τ_R	"	1.18 (1)	0.41	–
τ_{DB}	"	1.18 (1)	0.041	0.061
τ_{HB}	"	0.41 (2)	0.25	0.073
τ_R	"	0.41 (2)	1.59	–
τ_{DB}	"	0.41 (2)	0.08	0.35
τ_{HB}	"	1.30 (3)	0.22	0.15
τ_R	"	1.30 (3)	2.02	–
τ_{DB}	"	1.30 (3)	0.12	0.067
τ_{HB}	Aq. I^-	1.22 (1)	0.30	0.15
τ_R	"	1.22 (1)	2.21	–
τ_{DB}	"	1.22 (1)	0.05	0.062
τ_{HB}	"	0.43 (2)	0.36	0.11
τ_R	"	0.43 (2)	1.23	–
τ_{DB}	"	0.43 (2)	0.11	0.37
τ_{HB}	"	1.33 (3)	0.25	0.16
τ_R	"	1.33 (3)	2.41	–
τ_{DB}	"	1.33 (3)	0.10	0.057

- **The strength of HB bond is low at the supercritical condition w.r.t the results obtained at ambient condition.**
- **Polarity of the Sc-water will be different and that will effect the hydrophilic property of liq. Water at the Sc condition.**
- **The ion-water hydrogen bond is stronger in case of I^- ion.**
- **The water-water HB bond is effected more in case of the I^- ion w.r.t the Br^- ion.**

A. Karmakar, J. Mol. Liq., 279, 306-316 (2019)

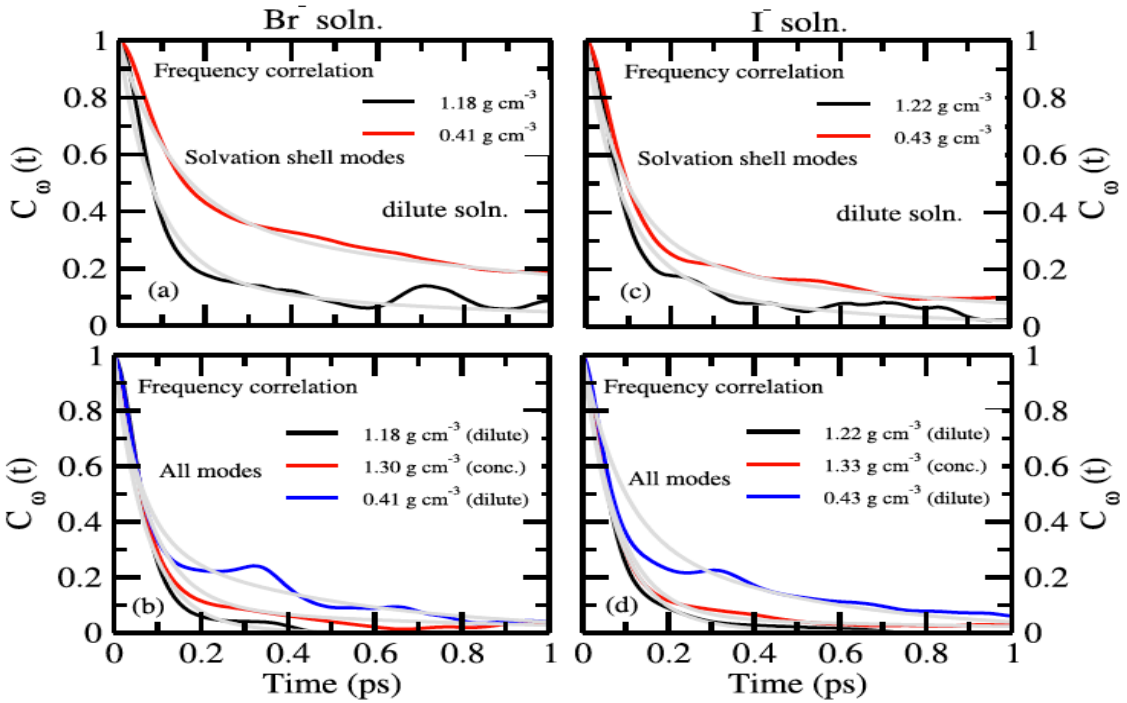

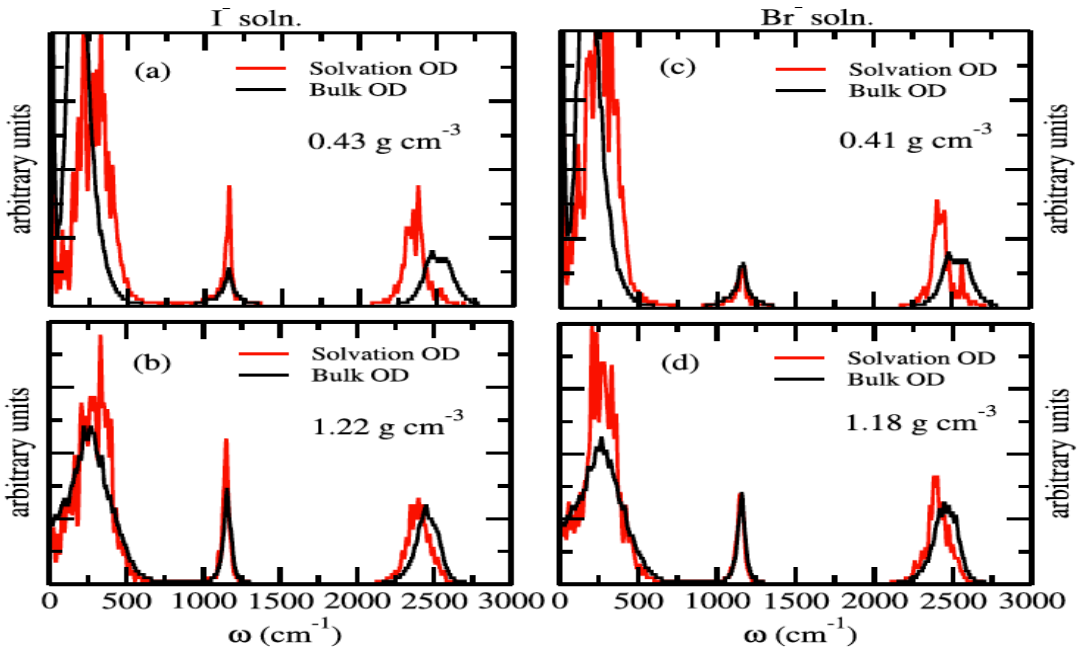

The calculated frequency-frequency time correlation has been fitted with a tri-exponential function $f(t) = b_1 e^{-\frac{t}{\tau_1}} + b_2 e^{-\frac{t}{\tau_2}} + b_3 e^{-\frac{t}{\tau_3}}$, where $b_1 + b_2 + b_3 = 1.0$ for the solvation shell OD modes while a bi-exponential function, $f(t) = b_1 e^{-\frac{t}{\tau_1}} + b_2 e^{-\frac{t}{\tau_2}}$, where $b_1 + b_2 = 1.0$, has been taken to fit the results for all OD modes.

Table 5
The time constants (weights) of frequency time correlation function of heavy water. The time constants are expressed in ps. Mass density has been used for heavy water (for convenience).

Quantity	Systems	Mass density (g cm^{-3})	Solvation shell modes	All modes
$\tau_1(b1)$	Aq. Br^-	1.18 (1)	0.08 (0.67)	0.07 (0.89)
$\tau_2(b2)$	"	1.18 (1)	0.18 (0.12)	0.14 (0.11)
$\tau_3(b3)$	"	1.18 (1)	0.41 (0.21)	–
$\tau_1(b1)$	"	0.41 (2)	0.12 (0.54)	0.06 (0.66)
$\tau_2(b2)$	"	0.41 (2)	0.25 (0.10)	0.45 (0.34)
$\tau_3(b3)$	"	0.41 (2)	1.46 (0.36)	–
$\tau_1(b1)$	"	1.30 (3)	–	0.08 (0.90)
$\tau_2(b2)$	"	1.30 (3)	–	0.77 (0.10)
$\tau_3(b3)$	"	1.30 (3)	–	–
$\tau_1(b1)$	Aq. I^-	1.22 (1)	0.07 (0.63)	0.07 (0.90)
$\tau_2(b2)$	"	1.22 (1)	0.15 (0.20)	0.17 (0.10)
$\tau_3(b3)$	"	1.22 (1)	0.48 (0.17)	–
$\tau_1(b1)$	"	0.43 (2)	0.09 (0.70)	0.09 (0.60)
$\tau_2(b2)$	"	0.43 (2)	0.36 (0.12)	0.43 (0.40)
$\tau_3(b3)$	"	0.43 (2)	1.14 (0.18)	–
$\tau_1(b1)$	"	1.33 (3)	–	0.08 (0.94)
$\tau_2(b2)$	"	1.33 (3)	–	1.04 (0.06)
$\tau_3(b3)$	"	1.33 (3)	–	–

- **Spectral diffusion in the solvation shell of the ion shows complicated dynamics through several decay channels.**
- **The ion-water hydrogen bond dynamics gets slower from high to low density solution and from Br^- to I^- ions.**
- **The interacting nature of ion-water is found to show opposite behavior at the supercritical condition**

A. Karmakar, J. Mol. Liq., 279, 306-316 (2019)

Aqueous Azide Ion Solutions at ambient condition

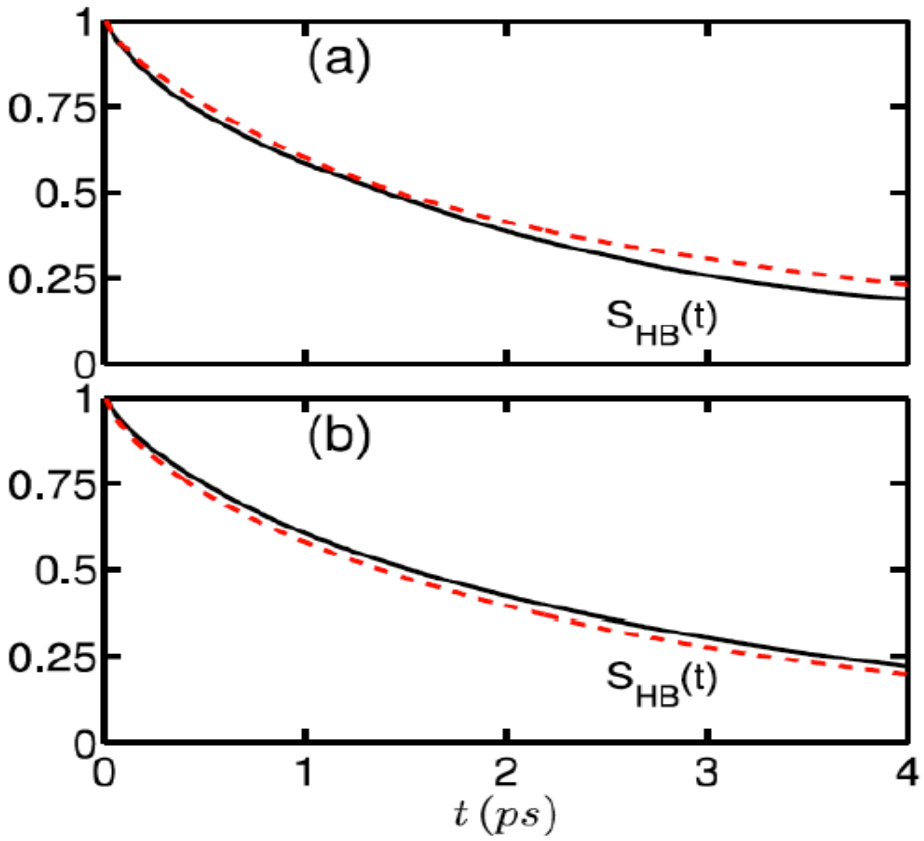

FIG. 5. The time dependence of the continuous hydrogen bond correlation function ($S_{HB}(t)$) of dilute solution (system 1). The results of (a) are for only N_3^--water hydrogen bonds and those of (b) are for all the hydrogen bonds present in system. The dashed curve is for the BLYP-D functionals and the solid curve is for the BLYP functional.

TABLE I. Average lifetimes of azide ion-water and all HBs of the relatively dilute (system 1) and concentrated (system 2) solutions for the BLYP functional. Results for residence times of water in ion hydration shell are also included. The results shown in brackets are for the BLYP-D functional. All time constants are expressed in picoseconds.

Quantity	System	Ion-water HBs	All HBs
τ_{HB}	1	2.43(2.52)	2.55(2.42)
τ_R	1	10.05(11.1)	...
τ_{HB}	2	1.97(1.04)	1.92(1.50)
τ_R	2	20.2(15.2)	...

TABLE II. Orientational relaxation times of the azide ion, water molecules inside and outside the solvation shell of the dilute solution (system 1) at ambient condition for the BLYP functional. The results shown in brackets are for the BLYP-D functional. The units are in ps.

Molecule	System	τ_2^{ori}
N_3^-	1	7.1(10.1)
D_2O (solv)	1	4.65(4.23)
D_2O (bulk)	1	4.48(3.66)

- **Azide – ion water HB strength are of the same order of water –water HB strength.**
- **Faster HB dynamics observed with increasing concentration**

A. Karmakar and A. Chandra, J. Chem. Phys. 2015, 142 (16), 1654505-10

Spectral diffusion of liquid water in the vicinity of azide ion in dilute solution

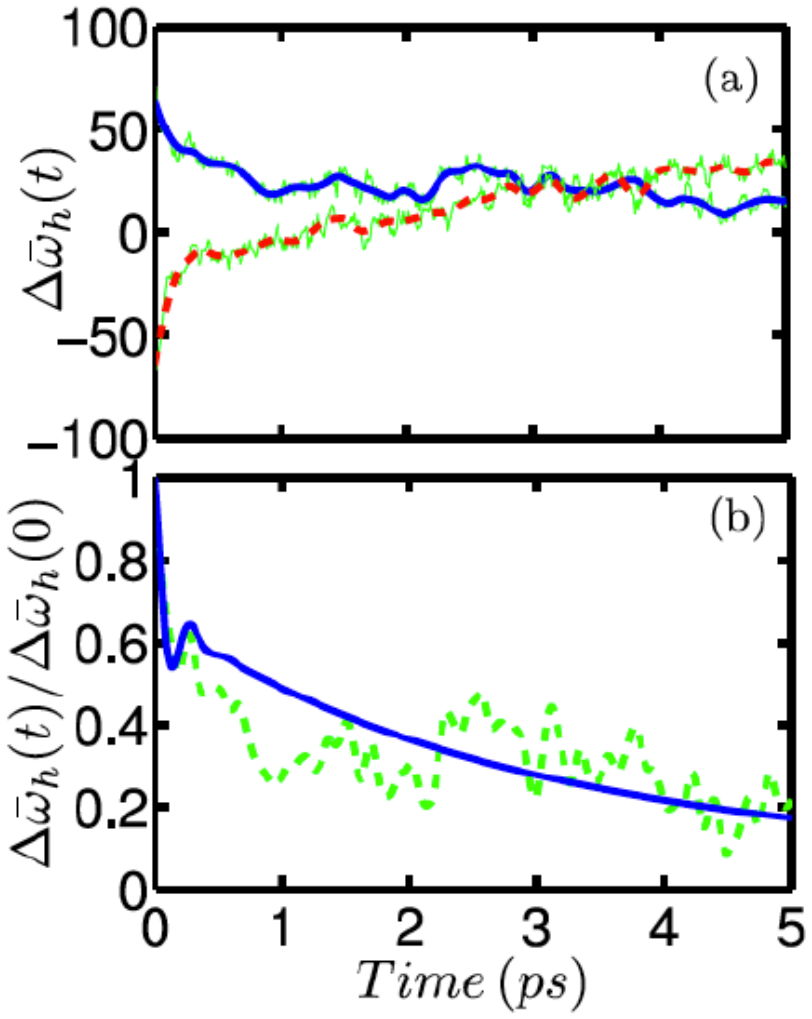

FIG. 6. The time dependence of the (a) average frequency shifts of the hole modes after excitations in blue and in red of the hydration shell OD modes when the hydration shell corresponds to that around a terminal nitrogen. The corresponding results for the blue excitation after normalization by the initial frequency shift are shown in (b). The solid and dashed curves correspond to excitations in blue and red, respectively. The smooth solid curve in (b) represents the fit by a function of Eq. (6). The results are for the dilute solution (system 1) and for the BLYP functional.

Spectral diffusion: $$f(t) = a_0 \cos(\omega_S t) e^{-\frac{t}{\tau_0}} + a_1 e^{-\frac{t}{\tau_1}} + (1 - a_0 - a_1) e^{-\frac{t}{\tau_2}}$$

Quantity	System	Excitation	τ_0	τ_1	τ_2	ω_S	a_0	a_1
$\Delta\bar{\omega}_h(t)$	1	Blue	0.10	2.43	10.12	101.91	0.33	0.50
$\Delta\bar{\omega}_r(t)$	1	Red	0.11	2.54	12.22	153.83	0.18	0.30
$\Delta\bar{\omega}_h(t)$	3	Blue	0.14	2.56	10.93	117.10	0.30	0.62
$\Delta\bar{\omega}_r(t)$	3	Red	0.11	2.72	12.81	123.61	0.28	0.45

- **Spectral diffusion of heavy water inside the solvation shell of azide ion appears as a complicated process.**
- **Spectral diffusion is found to decay with several other decay channels, such as through intact ion-water motion, hydrogen bond dynamics, orientational relaxation and residence dynamics.**
- **Inclusion of dispersion interaction is found to produce a faster vibrational spectral diffusion.**

A. Karmakar and A. Chandra, J. Chem. Phys. 2015, 142 (16), 1654505-10

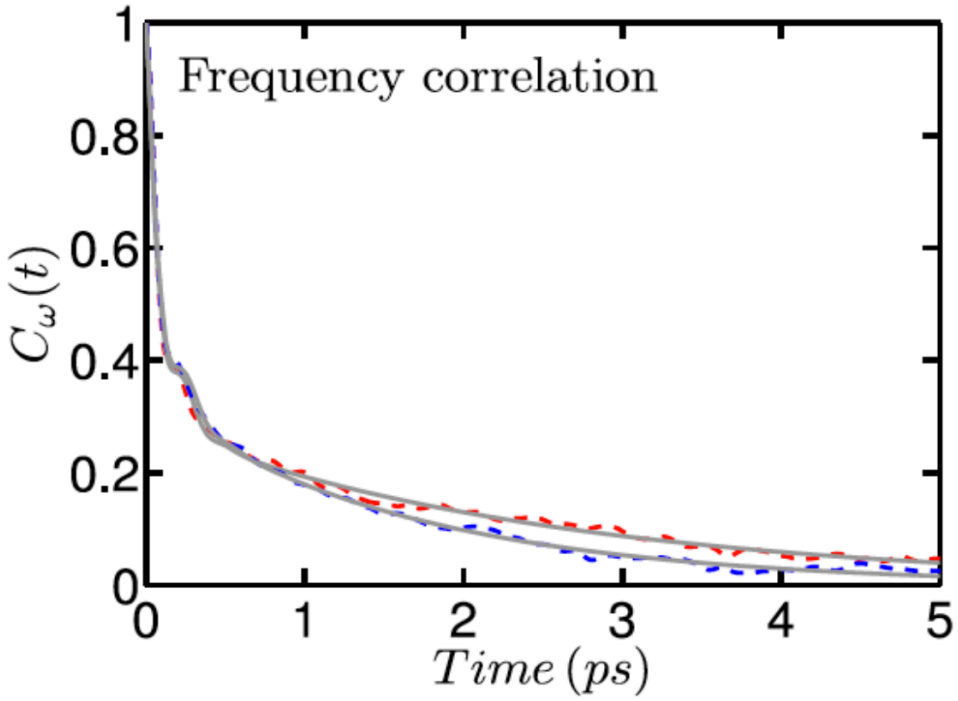

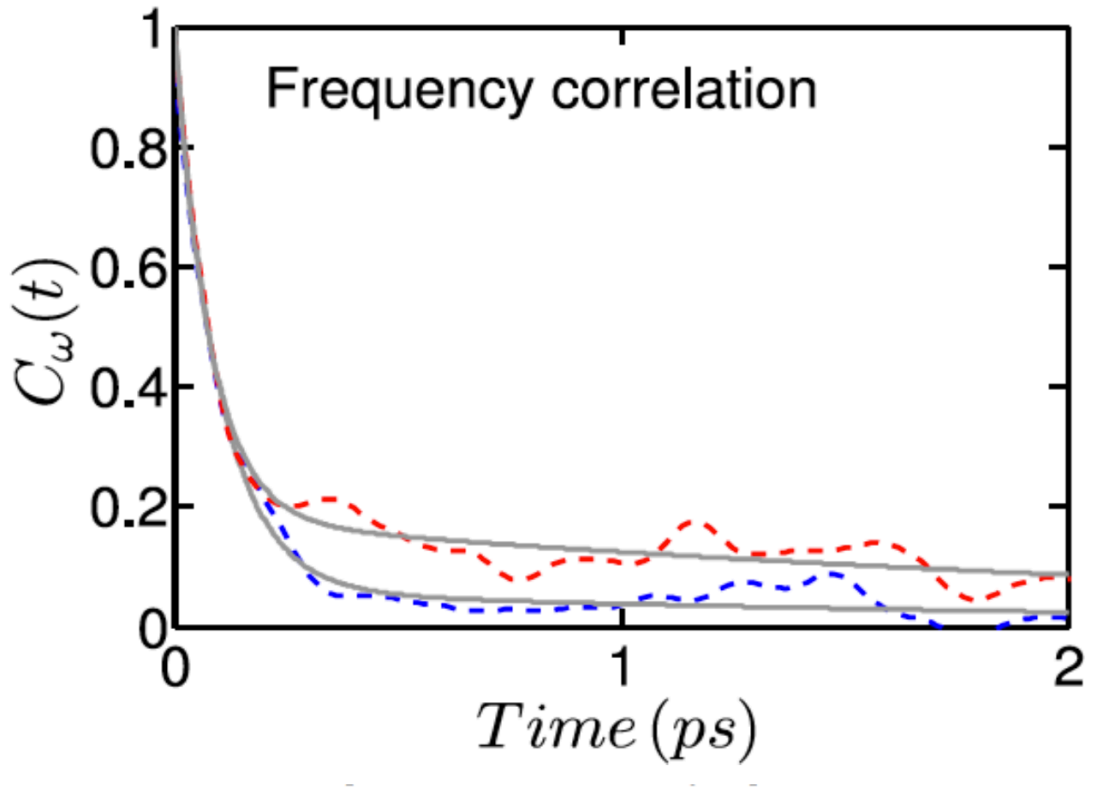

Quantity	Systems	Excitation	τ_0	τ_1	τ_2	ω_S	a_0	a_1
$C_\omega(t)$	1	…	0.06	0.16	2.75	152.81	0.31	0.38
$C_\omega(t)$	3	…	0.12	0.15	1.72	109.85	0.20	0.48

- Spectral diffusion of bulk water occurs via hydrogen bond decay channel.
- The effect of ion is local.

Quantity	System	Functional	τ_0	τ_1	a_0
$C_\omega(t)$	1	BLYP(BLYP-D)	0.079(0.10)	2.63(2.19)	0.85(0.94)
$C_\omega(t)$	2	BLYP(BLYP-D)	0.078(0.08)	0.66(0.59)	0.88(0.85)

- Spectral diffusion of azide ion occurs via hydrogen bond decay channel.
- The first short time scale stands for intact ion-water motion

A. Karmakar and A. Chandra, J. Chem. Phys. 2015, 142 (16), 1654505-10

Aqueous Azide Ion Solutions at supercritical condition

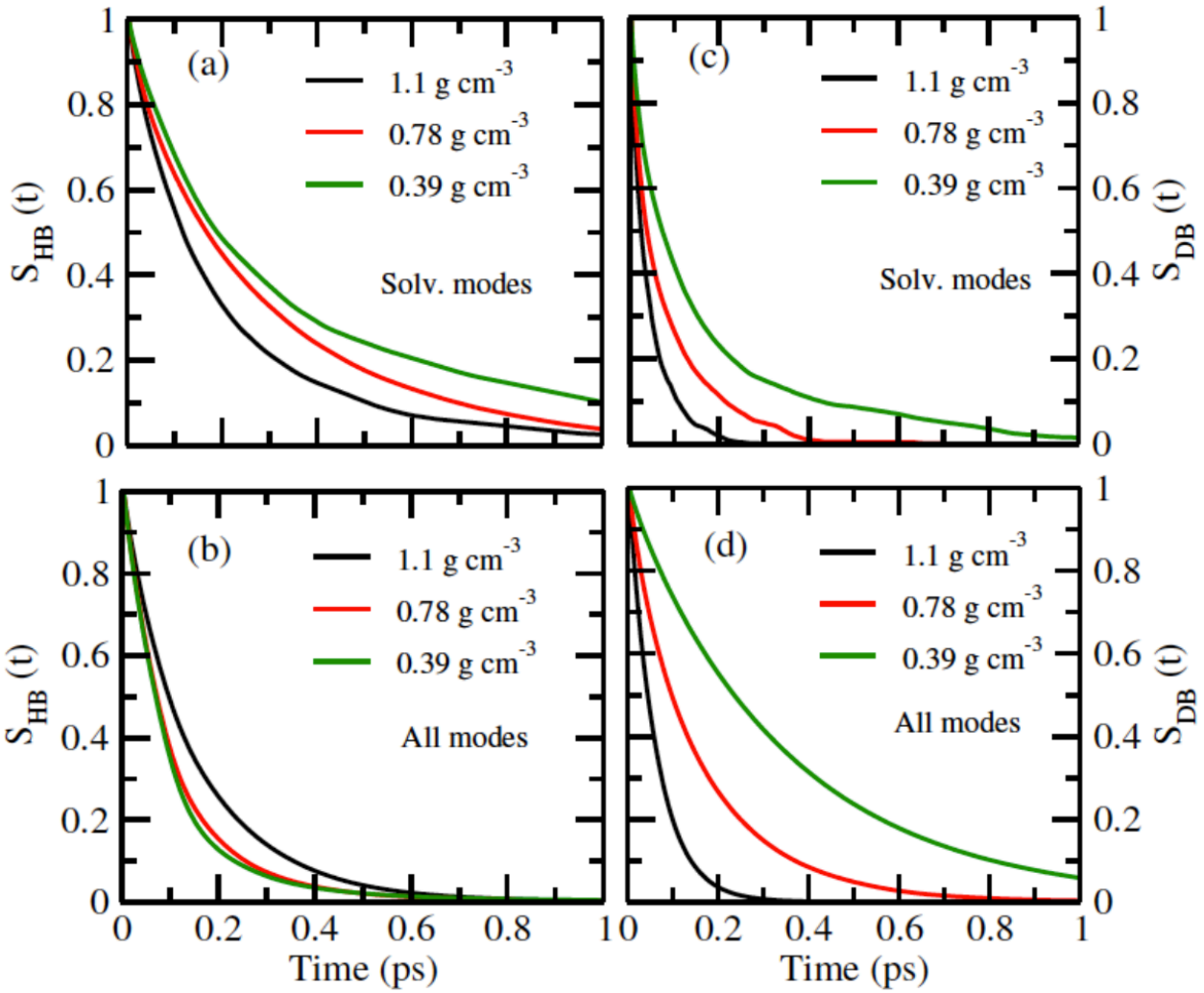

Figure 6: Hydrogen bond dynamics inside the solvation shell and for all OD modes for aqueous N_3^- solution at three different densities have been shown in (a) and (b), respectively. Dangling OD bond dynamics inside the solvation shell and for all OD modes for aqueous N_3^- solution at three different densities have been shown in (c) and (d), respectively. The density corresponds to the heavy water.

TABLE II. The average lifetimes of hydrogen bonds, residence times and dangling l water molecules in anion hydration shells and for all modes. All time scales are exp in ps. Mass density has been used for heavy water (for convenience). The detail simulating systems at 673 K and for BLYP functional.

Quantity	Systems	Mass density (g cm^{-3})	Solv. modes	All modes
τ_{HB}	Aq. N_3^-	1.1 (1)	0.21	0.19
τ_R	"	1.1 (1)	0.56	–
τ_{DB}	"	1.1 (1)	0.04	0.07
τ_{HB}	"	0.78 (2)	0.37	0.16
τ_R	"	0.78 (2)	0.72	–
τ_{DB}	"	0.78 (2)	0.15	0.08
τ_{HB}	"	0.39 (3)	0.36	0.09
τ_R	"	0.39 (3)	0.77	–
τ_{DB}	"	0.39 (3)	0.16	0.34

- **The water-water HB bond is effected more at lower density.**
- **Stochastic interaction will be less at lower density between the hydrogen bond forming sites.**
- **Local density effect is well captured using the model.**

A. Karmakar, J. Comp. Chem., Under Review, 2019

Spectra diffusion of Sc water in the vicinity of azide ion

TABLE III. The time constants (weights) of frequency time correlation function of heavy water. The time constants are expressed in ps. Mass density has been used for heavy water (for convenience). The details of all simulating systems at 673 K and for BLYP functional. The result at the ambient condition (298 K) has been taken from Ref. 40.

Quantity	Systems	Temperature	Mass density (g cm^{-3})	Solv. modes	All modes
$\tau_1(b1)$	Aq. N_3^-	673 K	1.1 (1)	0.07 (0.57)	0.08 (0.91)
$\tau_2(b2)$	"	"	1.1 (1)	0.30 (0.33)	0.22 (0.09)
$\tau_3(b3)$	"	"	1.1 (1)	0.60 (0.10)	—
$\tau_1(b1)$	"	"	0.78 (2)	0.09 (0.54)	0.08 (0.87)
$\tau_2(b2)$	"	"	0.78 (2)	0.36 (0.30)	0.30 (0.13)
$\tau_3(b3)$	"	"	0.78 (2)	1.10 (0.16)	—
$\tau_1(b1)$	"	"	0.39 (3)	0.06 (0.44)	0.08 (0.52)
$\tau_2(b2)$	"	"	0.39 (3)	0.26 (0.10)	0.49 (0.48)
$\tau_3(b3)$	"	"	0.39 (3)	0.77 (0.46)	—
$\tau_1(b1)$	"	298 K	1.1	0.10 (0.33)	0.06 (0.31)
$\tau_2(b2)$	"	"	1.1	2.43 (0.50)	0.16 (0.38)
$\tau_3(b3)$	"	"	1.1	10.12 (0.17)	2.75 (0.31)
ω_S (cm^{-1})	"	"	1.1	101.91	152.81

- **The spectral diffusion of water molecule is a complicated phenomena in the solvation shell of azide ion.**
- **Spectral diffusion occurs in multiple decay channels: 1st short time scale stands for the inertial motion, 2nd long time scale stands for the life time of HB bond and 3rd time scale corresponds to the residence dynamics.**
- **For all modes, spectral diffusion for high density: 1st short time scale is for inertial motion and the 2nd time scale corresponds to the water – water HB dynamics.**
- **For low density dilute solution, the observations are reversed for all modes**

A. Karmakar, J. Comp. Chem., Under Review, 2019

Spectra diffusion of of azide ion

TABLE IV. The time constants (weights) of frequency time correlation function stretch mode of azide ion. The details of all simulating systems at 673 K and for functional. The densities are calculated for heavy water with hydrogen mass of deut for convenience. The result at the ambient condition (298 K) has been taken fro Ref. 40.

Quantity	Systems	Temperature	Mass density (g cm^{-3})	Time (ps)
$\tau_1(b1)$	Aq. N_3^-	673 K	1.1 (1)	0.05 (0.41)
$\tau_2(b2)$	"	"	1.1 (1)	0.34 (0.59)
$\tau_1(b1)$	"	"	0.78 (2)	0.06 (0.21)
$\tau_2(b2)$	"	"	0.78 (2)	0.36 (0.79)
$\tau_1(b1)$	"	"	0.39 (3)	0.05 (0.86)
$\tau_2(b2)$	"	"	0.39 (3)	0.24 (0.14)
$\tau_1(b1)$	"	298 K	1.1	0.08 (0.85)
$\tau_2(b2)$	"	"	1.1	2.63 (0.15)

- **The spectral diffusion of azide ion is a complicated phenomena.**
- **Spectral diffusion occurs in multiple decay channels: 1st short time scale stands for the inertial motion and 2nd long time scale stands for the life time of HB bond for all cases.**

A. Karmakar, J. Comp. Chem., Under Review, 2019

Electric field fluctuation of azide ion and Sc-water

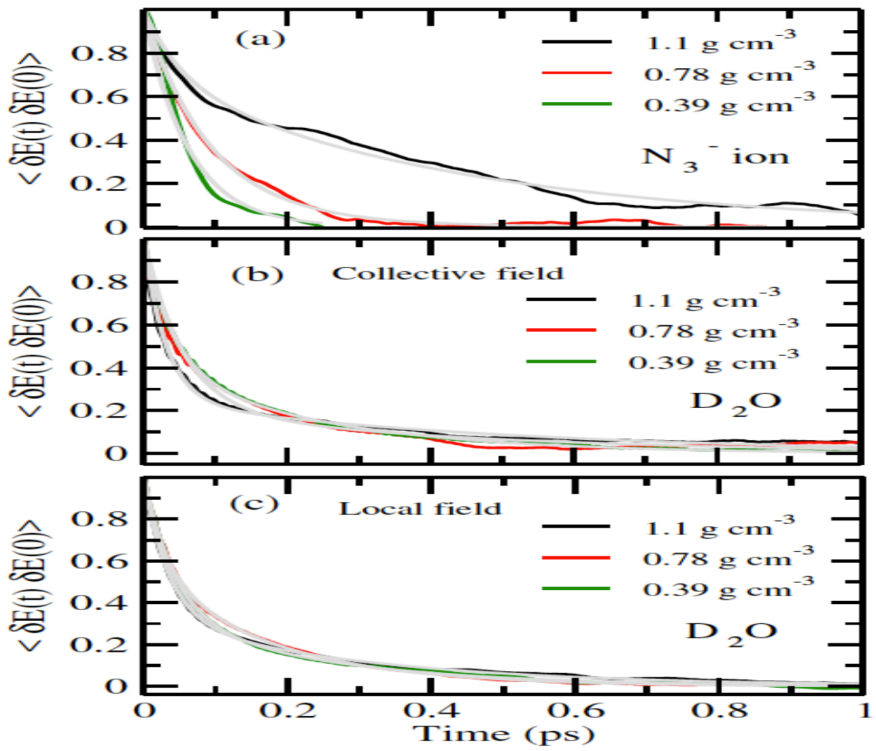

9: The fluctuating electric field on nitrogen atom of azide ion due to the collective f ion has been shown in (a). The fluctuating electric field on deuterium atom of water for both the collective and local field of the solvent molecules have been in (b) and (c), respectively at three different densities. The grey curve is for the data. The density corresponds to the heavy water.

TABLE V. The time constants (weights) of electric field fluctuations on deuterium of heavy water. The details of all simulating systems at 673 K and for BLYP func The time constants are expressed in ps.

Quantity	Fields	Mass density (g cm^{-3})	Time (ps)
$\tau_1(b1)$	local	1.1 (1)	0.035 (0.67)
$\tau_2(b2)$	"	1.1 (1)	0.30 (0.33)
$\tau_1(b1)$	collective	1.1 (1)	0.03 (0.75)
$\tau_2(b2)$	"	1.1 (1)	0.48 (0.25)
$\tau_1(b1)$	local	0.78 (2)	0.03 (0.43)
$\tau_2(b2)$	"	0.78 (2)	0.17 (0.57)
$\tau_1(b1)$	collective	0.78 (2)	0.054 (0.78)
$\tau_2(b2)$	"	0.78 (2)	0.42 (0.22)
$\tau_1(b1)$	local	0.39 (3)	0.04 (0.67)
$\tau_2(b2)$	"	0.39 (3)	0.24 (0.33)
$\tau_1(b1)$	collective	0.39 (3)	0.04 (0.60)
$\tau_2(b2)$	"	0.39 (3)	0.24 (0.40)

TABLE VI. The time constants (weights) of electric field fluctuations on nitroger of azide ion. The details of all simulating systems at 298 K and 673 K and for functional. The densities are calculated for heavy water with hydrogen mass of deu for convenience. The time constants are expressed in ps.

Quantity	Temperature	Mass density (g cm^{-3})	Time (ps)
$\tau_1(b1)$	673 K	1.1 (1)	0.05 (0.30)
$\tau_2(b2)$	"	1.1 (1)	0.42 (0.70)
$\tau_1(b1)$	"	0.78 (2)	0.09 (0.86)
$\tau_2(b2)$	"	0.78 (2)	0.15 (0.14)
$\tau_1(b1)$	"	0.39 (3)	0.06 (1)
$\tau_2(b2)$	"	0.39 (3)	-
$\tau_1(b1)$	298 K	1.1	0.09 (0.72)
$\tau_2(b2)$	"	1.1	2.22 (0.28)

- **The spectral diffusion data has been correlated with the dielectric fluctuation of the solvating medium for both the azide and water molecules.**
- **For the water molecules we observed a break down in the correlation of collective and local electric field fluctuations with increasing density.**
- **This finding has been confirmed by the calculated dipole moment values of water at the Supercritical condition.**
- **For the azide molecular ion, the effect of the ion is collective as it is a charged ion.**
- **The electric field fluctuations on the terminal nitrogen atom is due to the hydrogen bond dynamics of the surrounding water molecules.**

A. Karmakar, J. Comp. Chem., Under Review, 2019

Conclusion

1. First Principle methodology has been proposed to model the structure and dynamical properties of aqueous ionic solutions.

2. Structural dynamical properties have been correlated with the spectral diffusion data of the fluctuating aqueous ionic solutions.

3. The proposed first principle methodology was able to capture the hydrophobic and hydrophilic nature of the aqueous ionic solutions at different thermodynamic condition and was able to explain these behaviors from first principle study.

4. Aqueous iodide ion solution appeared as hydrophilic in nature w.r.t the aqueous bromide ion and aqueous azide ion solution at the supercritical condition.

5. The proposed model was able to explain the reason behind the observed Hofmeister series effect for Br^- and I^- ion in terms of ion-water interactions from the first principle study.

Acknowledgement

The research leading to these results has been funded by the Department of Science and Technology, India. The calculations have been run using High Performance Computational Facility at IIT Kanpur. AK would also like to thank her funding support in LANL through 20170046DR project.

सत्यमेव जयते

Department of Science & Technology, Government of India

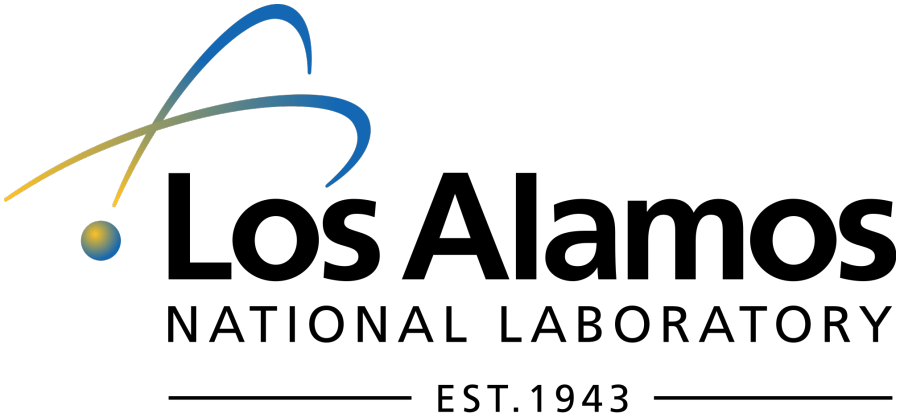

A theory guided approach towards the development of highly efficient redox flow cell

Anwesa Karmakar

Rangachary Mukundan, Ping Yang and Enrique R. Batista

Los Alamos National Laboratory

Funding Resources

Phys. Chem. Chem. Phys., Under Review, 2019

Motivation

- The redox flow batteries are highly popular as storage device.
- Widely used storage device in this field is aqueous Vanadium redox flow cell.
- Despite of their advantages they suffer from disadvantages.
- Non aqueous solvents have been getting importance because of their wide potential window.
- In redox flow cell, two important parameters are needed to be taken into consideration: Energy density and Power density (Second generation storage device)
- The energy density is directly related with the solubility of metal complex in non-aqueous media.
- In non-aqueous redox flow cell, the media are composed of organic solvent and ionic liquid as supporting electrolyte.

$V(acac)_3^+ + e^- \leftrightarrow V(acac)_3$ **(Catholyte)**

$V(acac)_3 + e^- \leftrightarrow V(acac)_3^-$ **(Anolyte)**

$V(acac)_3^+ + V(acac)_3^- \leftrightarrow 2V(acac)_3$ **Overall reaction**

Experimental Findings

- Common anions are expected in redox flow cell are $PF6^-$, $BF4^-$ and $Tf2N^-$ (found stable over a wide voltage window).
- Quaternary ammonium cations are the most common non-reactive species. Possibility of using large cation ionic liquid has been increasing if they are stable over an appropriate voltage window.
- For a successful redox flow cell compatible solvent/supporting electrolyte combination is most important thing. Main properties are needed to be handled
  - High active species solubility
  - High supporting electrolyte solubility
  - High solution conductivity
- Metal complex and supporting electrolyte usually will hold a duel solute relationship in redox flow cell.

A. A. shinkle *at al*; Journal of Power Sources 248 (2014) 1299-1305; Gong *at al.*; Energy Environ. Sci. 8 (2015)

Difficulties to solve the problem

- Metal Complex Solubility in Ionic Liquids
  - Molecular dynamics simulation via thermodynamic integration in DFT.
  - The calculations are computationally expansive, time consuming, demands specific expertise and thus not suitable for large scale industrial applications.
  - Solubility can be calculated using Stachard-Hildebrand, Hansen solubility parameters model and COSMO-RS but further statistical physics needed to be developed for metal complexes.

- Difficulties for Metal Complexes
  - No COSMORS/COSMOSAC parameters for metal and hence for metal complexes.
  - Direct implementation to any of these models is computationally expansive, time consuming and challenging.

Symmetric solution

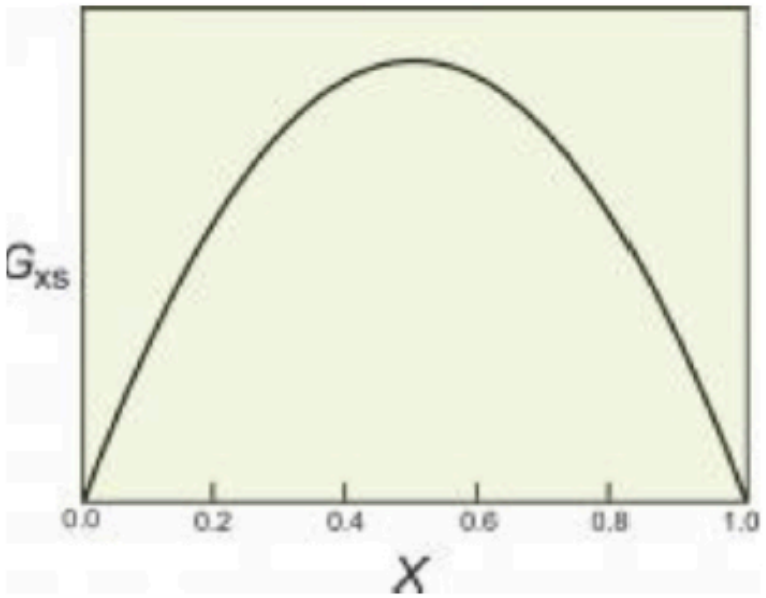

Asymmetric solution

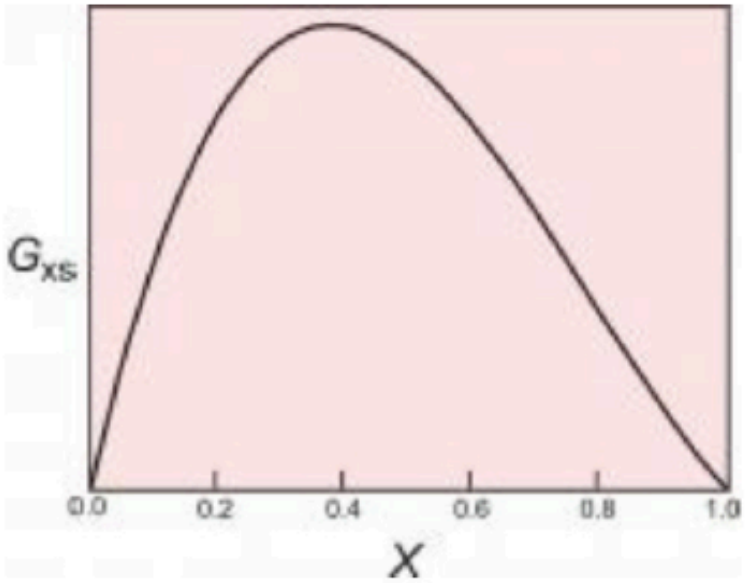

3-Suffix Margule Function

$$G^{ex} = \Delta G^{asym}_{i/S}(real) - \Delta G^{asym}_{i/i}(ideal) = x_1 x_2 (A_{21} x_1 + A_{12} x_2)$$

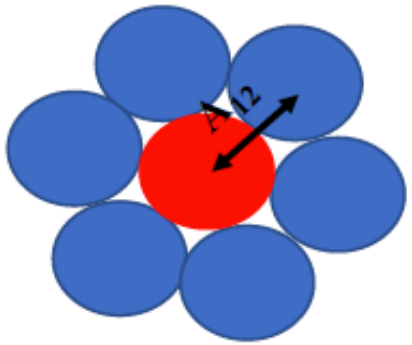

Species (1)

Species (2)

$$\ln\gamma_1 = \frac{\alpha_1 x_2^2 + \beta_1 x_2^3}{RT}$$

$$\ln\gamma_2 = \frac{\alpha_2 x_1^2 + \beta_2 x_1^3}{RT}$$

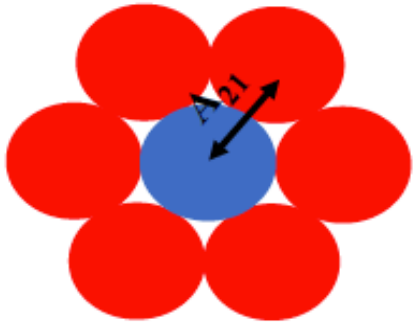

$A_{12} = RT\ln\gamma_{12}$, when $x_1 \longrightarrow 0$; $x_2 \longrightarrow 1$

$A_{21} = RT\ln\gamma_{21}$, when $x_2 \longrightarrow 0$; $x_1 \longrightarrow 1$

$A_{12} = A_{21}$, symmetric interaction

$A_{12} \neq A_{21}$, asymmetric interaction

Activity coefficient is the measurement of the non-ideality present in a solution

J. M. Prausnitz *et al. Molecular thermodynamics of fluid phase equilibria*, 3rd Ed.

Phys. Chem. Chem. Phys., Under Review, 2019

[1]Asymmetric model: $\ln\gamma = \ln\gamma_{LR}^{combinatorial} + \ln\gamma_{SR}^{asymmetric} \longrightarrow$ "LANL" activity coeffcient model

$\ln\gamma_{LR}^{combinatorial}$ = Stavermann − Guggeinheim Combinatorial term = $\frac{\mu_{LR}^{comb}(\sigma)}{RT}$ =

$$1 - \frac{\phi_i}{x_i} + \ln\frac{\phi_i}{x_i} - \frac{z}{2}q_i\left(1 - \frac{\phi_i}{\theta_i} + \ln\frac{\phi_i}{\theta_i}\right)$$

- ϕ_i = fraction volume; θ_i = fraction surface
- x_i = mole fraction of ith species; z = coordination number

$\ln\gamma_{SR}^{asymmetric} = \frac{\mu_{SR}^{asym}(\sigma)}{RT} = \frac{\alpha_i x_j^2 + \beta_i x_j^3}{RT} \longrightarrow$ for solute; $\frac{\alpha_j x_i^2 + \beta_j x_i^3}{RT} \longrightarrow$ for solvent

- $\alpha_i = \left(2A_{21} - A_{12}\right); \beta_i = \left(2A_{12} - 2A_{21}\right); \alpha_j = \left(2A_{12} - A_{21}\right); \beta_j = \left(2A_{21} - 2A_{12}\right)$
- $A_{12} = RT\ln\gamma_{asym}^{\infty}$, when $x_1 \to 0; x_2 \to 1$ $A_{21} = RT\ln\gamma_{asym}^{\infty}$, when $x_2 \to 0; x_1 \to 1$
- A_{12} and A_{21} are known as "Margule parameters"
- $\ln\gamma_{asym}^{\infty} = \ln\gamma_{LR}^{comb} + \ln\gamma_{SR}^{residual} + \ln\gamma^{dispersion}$; at infinite dilution
- x_i = mole fraction of solute; x_j = mole fraction of solvent

When Margules parameters will be imported from COSMOSAC model, the model will be referred as "COSMOSAC-LANL" model.

[1]A. Karmakar *et al.* (submitted).

Phys. Chem. Chem. Phys., Under Review, 2019

COSMOSAC-2013 model: $\ln\gamma = \ln\gamma_{LR}^{combinatorial} + \ln\gamma_{SR}^{residual} + \ln\gamma^{dispersion}$

$\ln\gamma_{LR}^{comb}(i/S) = \text{Stavermann} - \text{Guggeinheim Combinatorial term} = \frac{\mu_{LR}^{comb}(\sigma)}{RT} =$

$1 - \frac{\phi_i}{x_i} + \ln\frac{\phi_i}{x_i} - \frac{z}{2}q_i\left(1 - \frac{\phi_i}{\theta_i} + \ln\frac{\phi_i}{\theta_i}\right)$

- ϕ_i = fraction volume = $\frac{x_i r_i}{\sum_j x_j r_j}$; θ_i = fraction surface = $\frac{x_i q_i}{\sum_j x_j q_j}$
- x_i = mole fraction of ith species; z = coordination number

$\ln\gamma_{SR}^{residual} = \frac{\mu_{SR}^{residual}(\sigma)}{RT} = \ln\Gamma_S^t(\sigma_m^t) = -\ln\left\{\sum_S^{nhb,hb}\sum_{\sigma_n} p_S^s(\sigma_n^s)\Gamma_S^s(\sigma_n^s)exp\left(-\frac{\Delta W(\sigma_m^t,\sigma_n^t)}{RT}\right)\right\}$

- $\Gamma_S^t(\sigma_m^t)$=total segment activity coefficient
- p_S^S = Sigmaprofile of mixture
- $\Delta W(\sigma_m^t, \sigma_n^t)$ = exchange interaction between segments

$A_{mix}^{dispersion} = -\frac{\sum_i\sum_j\sum_{\alpha\in i}\sum_{\beta\in j} x_i x_j E_{\alpha\beta}}{V_{mix}}$; $\left(\frac{\partial n A_{mix}^{disp}/RT}{\partial n_i}\right)_{T,V,i\neq j} = \ln\gamma^{dispersion}$; $E_{\alpha\beta} = \sqrt{\varepsilon_\alpha\varepsilon_\beta}m_\alpha m_\beta$

- $\sqrt{\varepsilon_\alpha\varepsilon_\beta}$=pair interaction energy
- m_α & m_β = effective number of atom of types α & β, respectively
- V_{mix} = molar volume of the mixture

R. Xiong *et al. Ind. Chem. Res. Eng.* 53, 2014 (8265-8278).

Phys. Chem. Chem. Phys., Under Review, 2019

Information obtained from quantum COSMO calculation

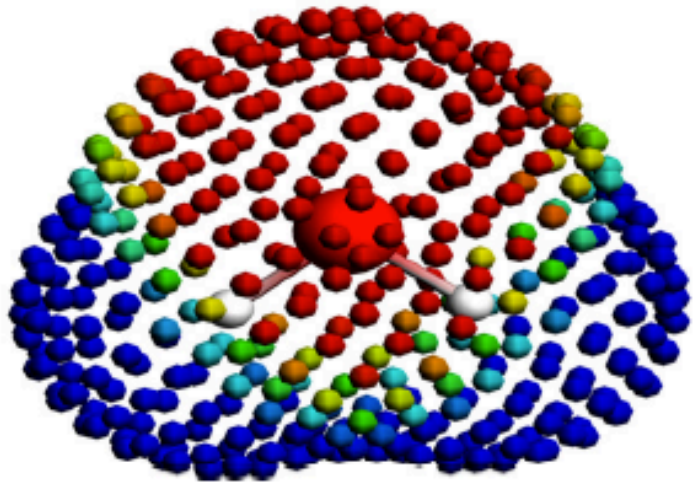

COSMO surface points

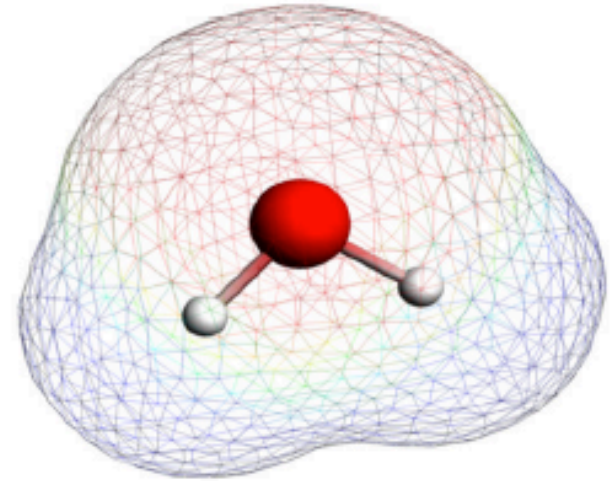

COSMO Surface $A_i(\sigma)$

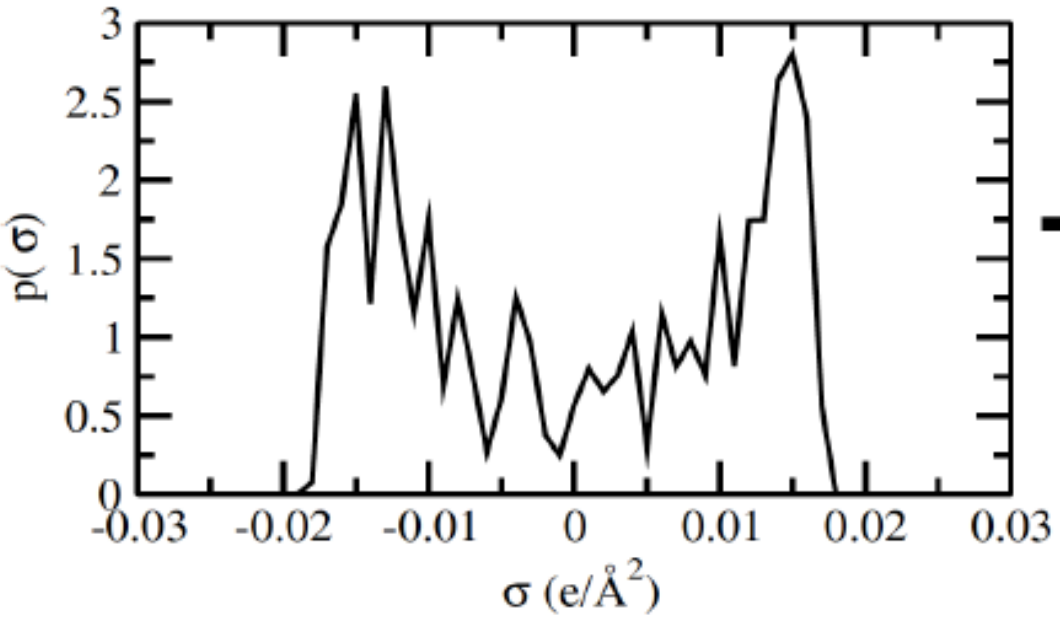

Sigmaprofile $p_i(\sigma)$

Sigmaprofile is an unique property of a compound and provides activity coefficient (γ)

Phys. Chem. Chem. Phys., Under Review, 2019

COSMO Surface of Metal Complex and Group contribution method

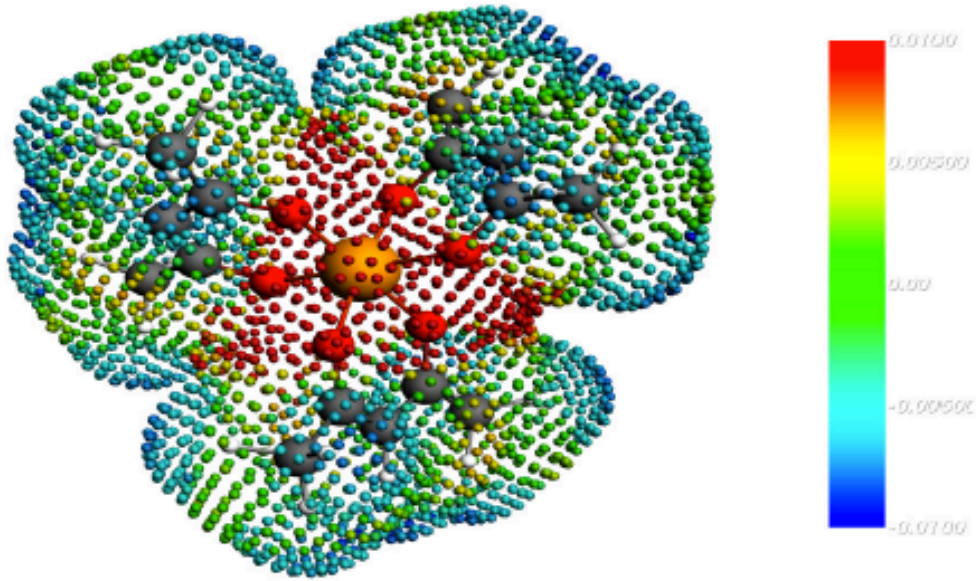

Figure 1: COSMO surface points of $V(acac)_3$

Unrestricted calculation for Metal complex

V^{3+} is [Ar] $4s^0$ $3d^2$

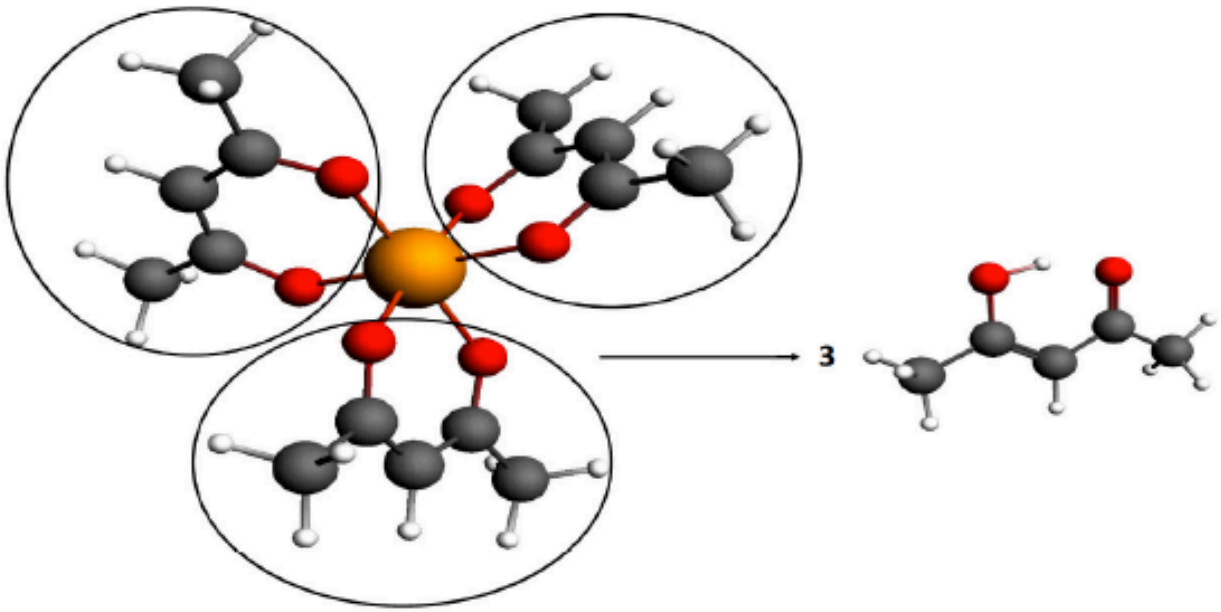

Figure 2: Proposed GCM model for metal complex

A. Karmakar *et al.* (submitted).

Phys. Chem. Chem. Phys., Under Review, 2019

Extension of Application to Metal Complexes (Same types of ligands)

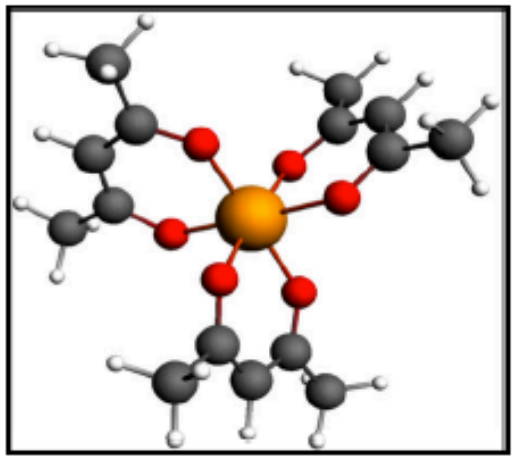

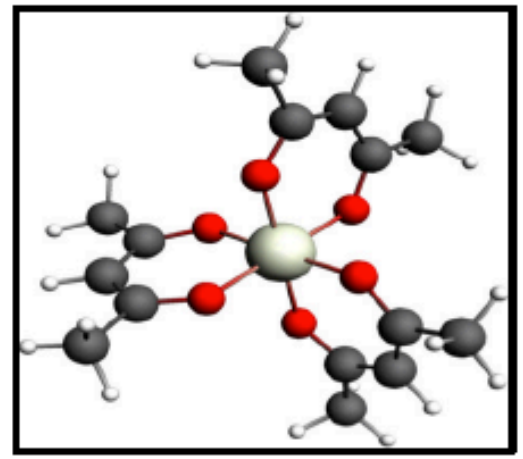

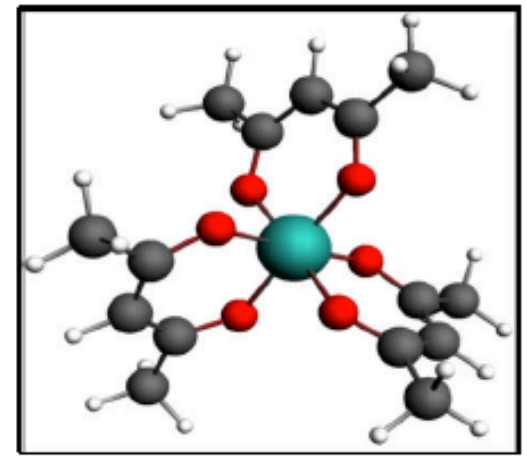

$V(acac)_3$ (I) | **$Cr(acac)_3$ (II)** | **$Mn(acac)_3$ (III)**

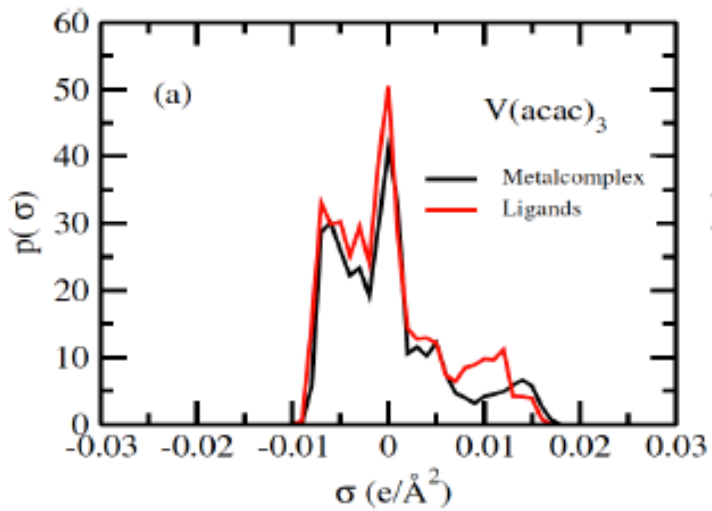

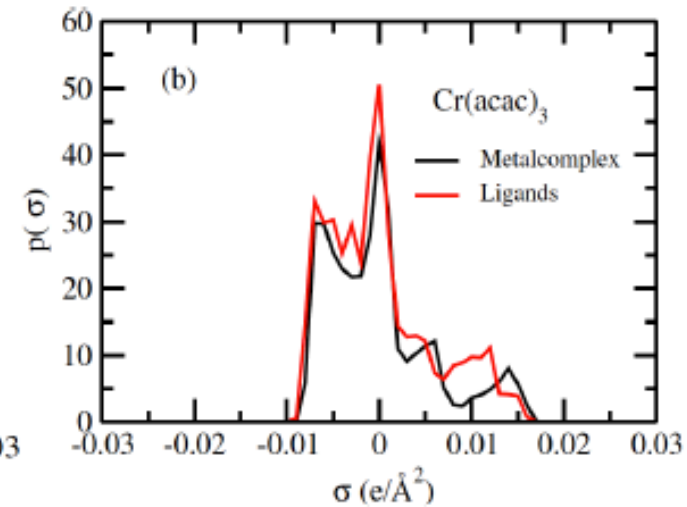

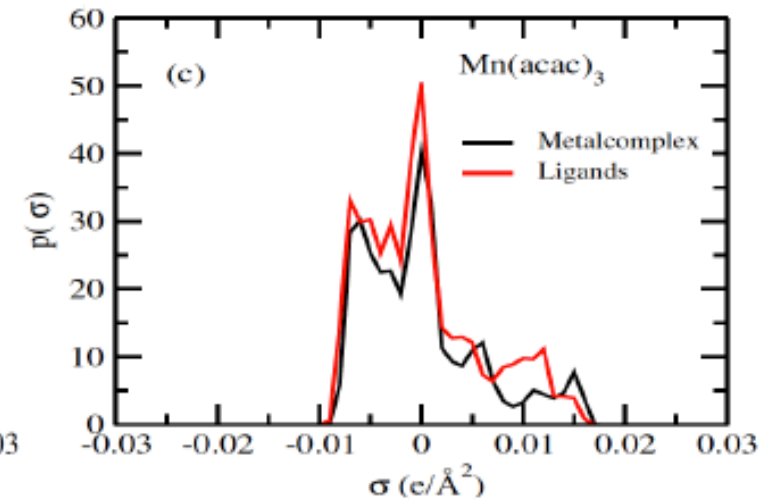

Thus, the electron configuration of Cr^{3+} is:
$Cr^{3+}: 1s^2 2s^2 2p^6 3s^2 3p^6 4s^0 3d^3$

The electron configuration for a Mn^{3+} ion is $[Ar]3d^4$.

A. Karmakar *et al.* (submitted).

Phys. Chem. Chem. Phys., Under Review, 2019

Extension of Application to Metal Complexes (Same types of ligands)

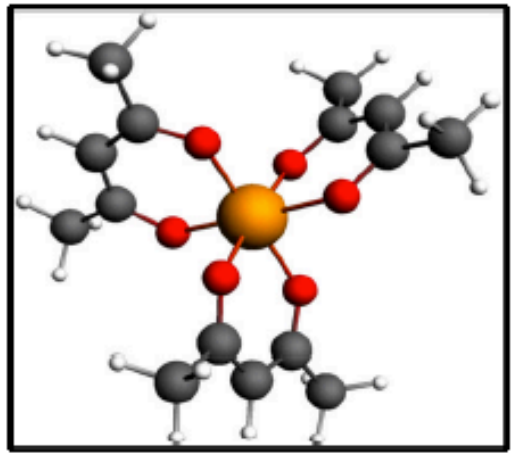

$V(acac)_3$ (I)

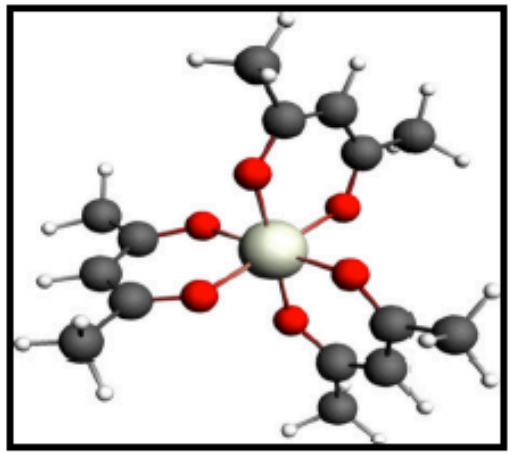

$Cr(acac)_3$ (II)

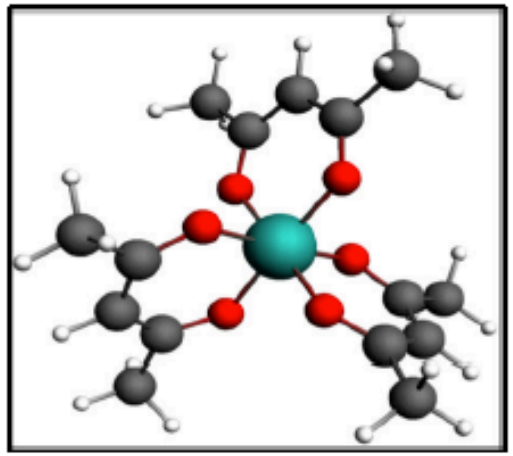

$Mn(acac)_3$ (III)

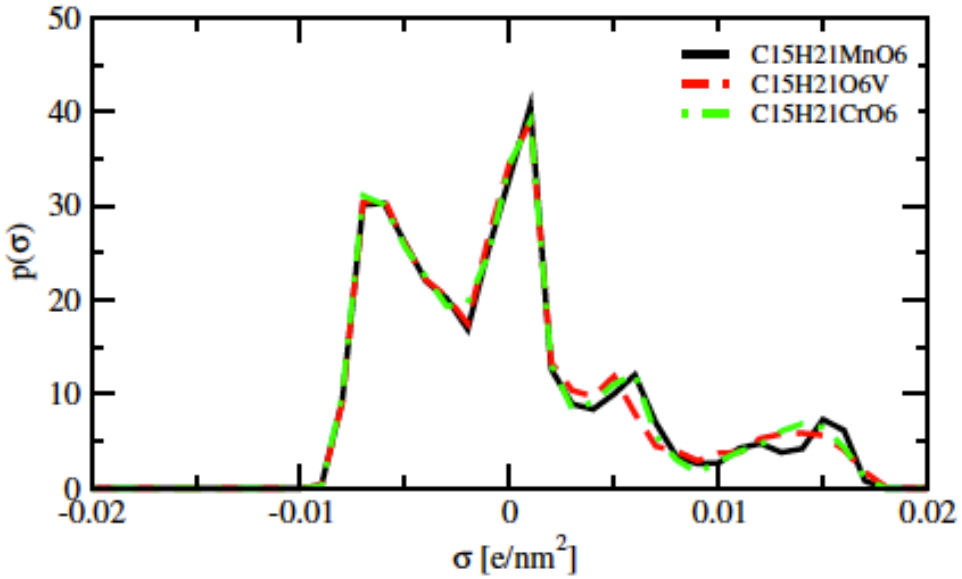

Solubility Order III ≃ I < II

Sigmaprofile can be correlated qualitatively with the solubility order of metal complex

Metal Complex's sigmaprofile is function of sigmaprofile of ligands

A. Karmakar *et al.* (submitted); J. Mat. Chem. A , 2015, 3, 7929-7938

Phys. Chem. Chem. Phys., Under Review, 2019

Extension of Application to Metal Complexes (Different types of ligands)

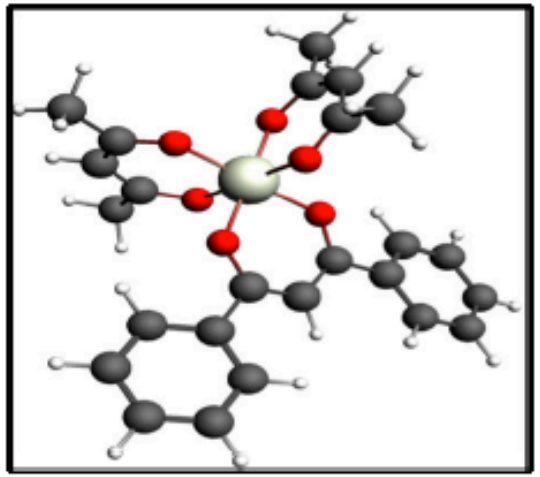

$Cr(acac)_2acacph_2$ (IV)

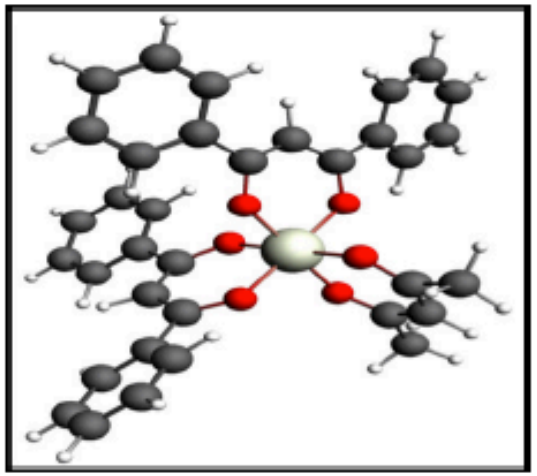

$Cracac(acacph_2)_2$ (V)

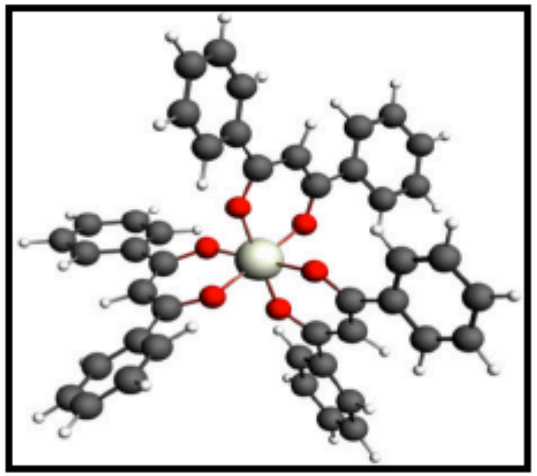

$Cr(acacph_2)_3$ (VI)

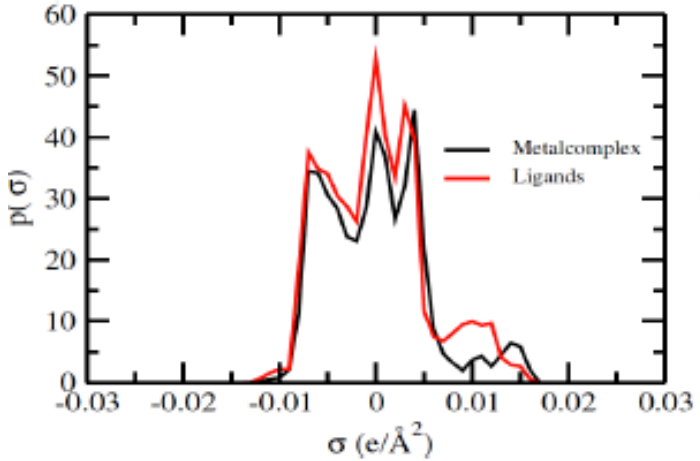

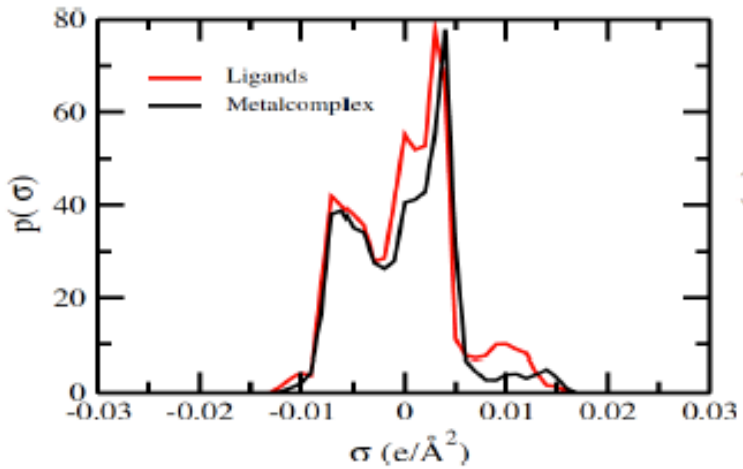

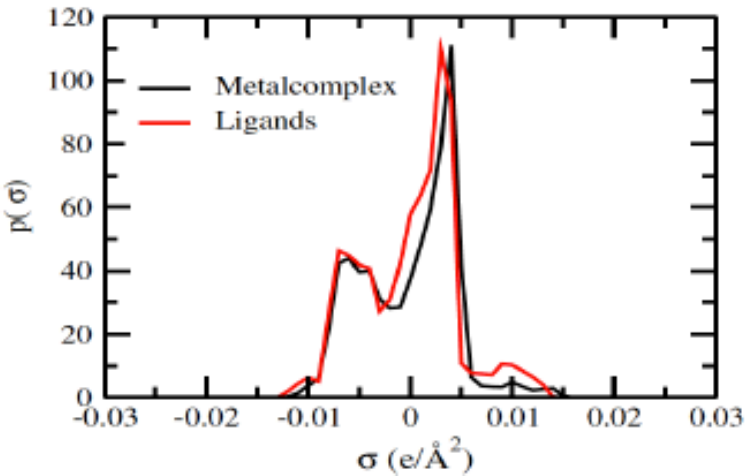

Sigmaprofiles are different for a metal complex with different ligands

A. Karmakar *et al.* (submitted).

Phys. Chem. Chem. Phys., Under Review, 2019

Extension of Application to Metal Complexes (Different types of ligands)

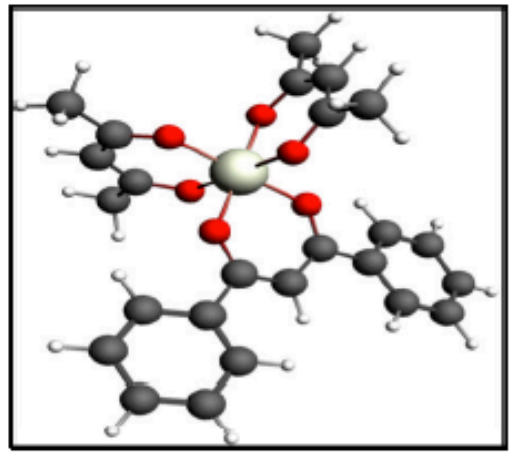

$Cr(acac)_2acacph_2$ (IV)

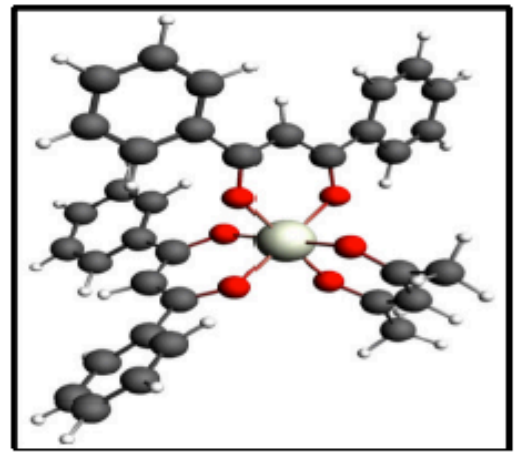

$Cracac(acacph_2)_2$ (V)

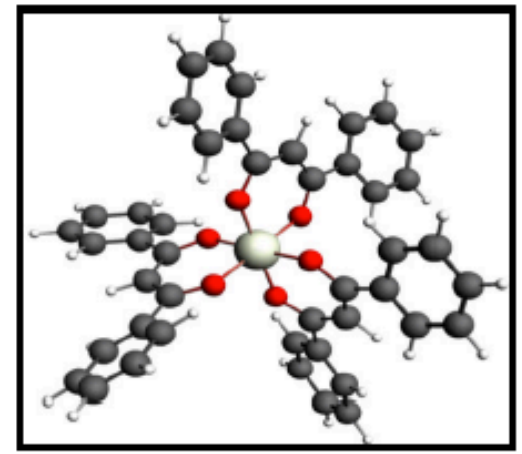

$Cr(acacph_2)_3$ (VI)

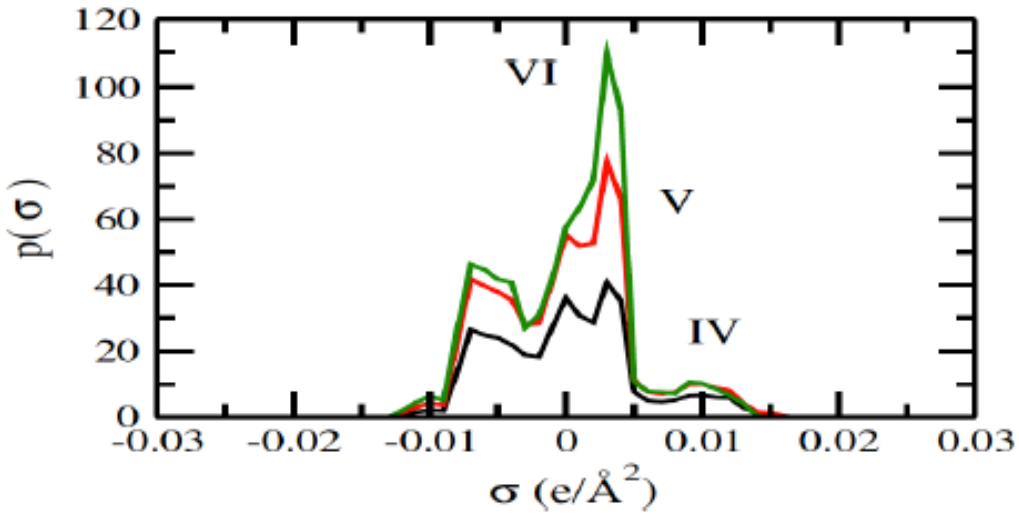

Solubility Order VI< V < IV

Sigmaprofile can be correlated qualitatively with the solubility order of metal complex

Sigmaprofiles are different for a metal complex with different ligands

A. Karmakar *et al.* (submitted); J. Mat. Chem. A , 2015, 3, 7929-7938

Phys. Chem. Chem. Phys., Under Review, 2019

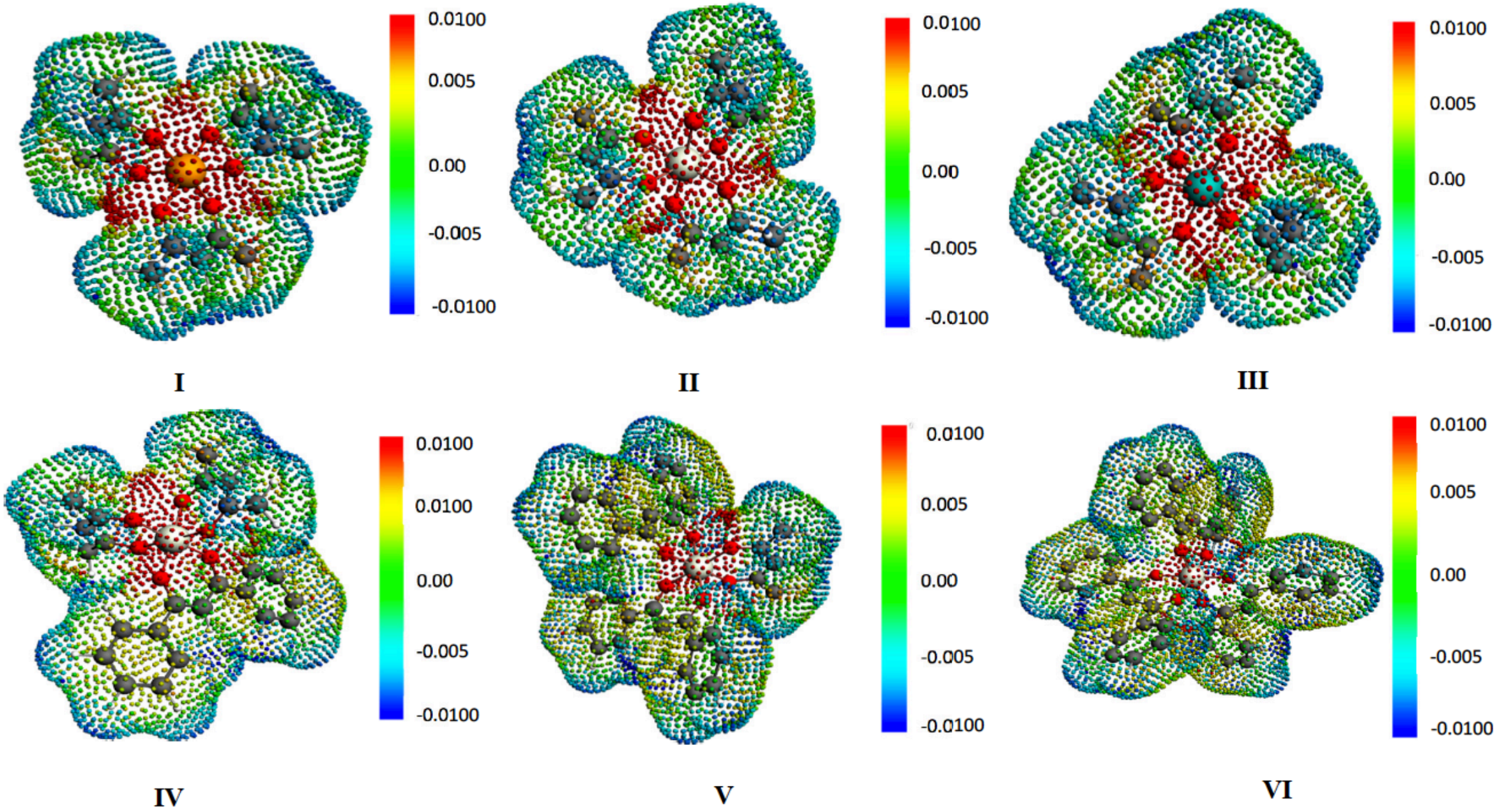

Ligand induced charge density is reducing on the metal center upon decreasing the solubility of it in Acetonitrile

Phys. Chem. Chem. Phys., Under Review, 2019

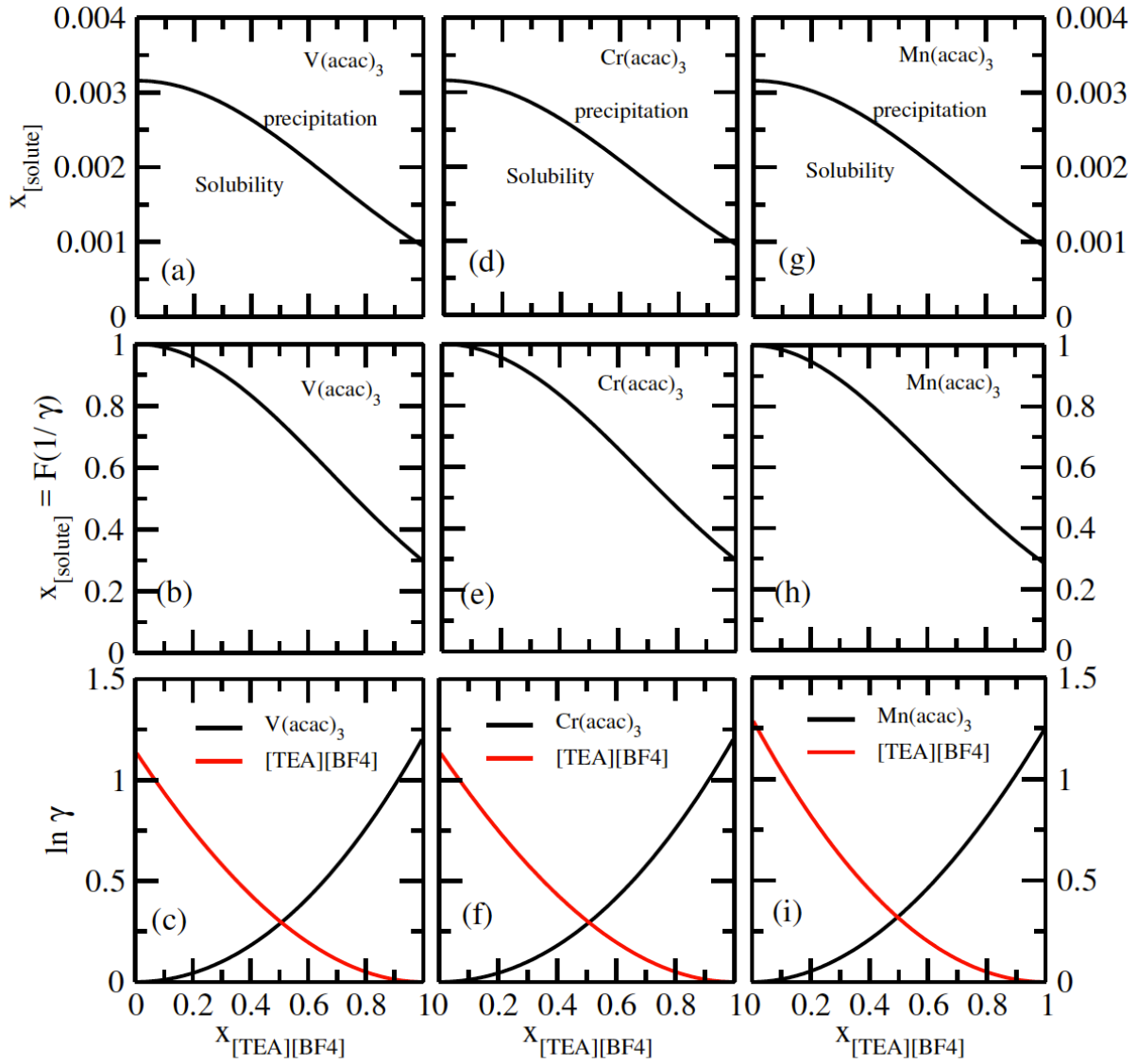

Figure 14: The calculated phase diagrams have been shown in figs. (a) and (b) for $V(acac)_3$, in figs. (d) and (e) for $Cr(acac)_3$ and in figs. (g) and (h) for $Mn(acac)_3$metal complexes. In figs. (c), (f) and (i), the Gibbs-Duhem relationship for the three binary systems have been shown.

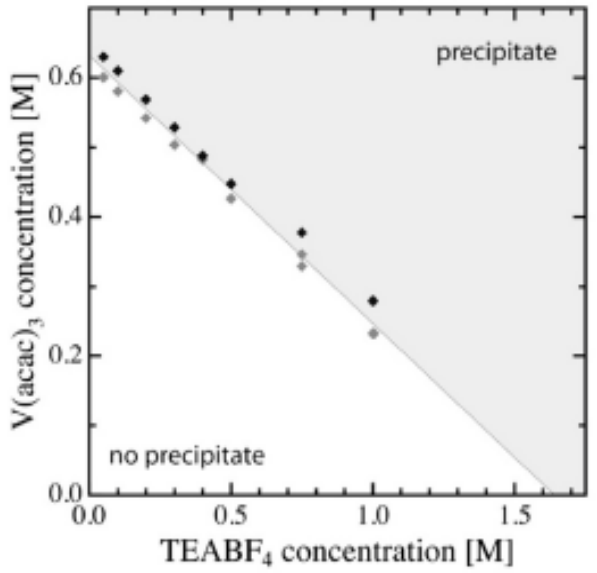

Phase diagram that establishes the maximum solubility of $V(acac)_3$ active as a function of $TEABF_4$ concentration in ACN at room temperature. Light points compositions where both solutes dissolved; dark points show target com- s where precipitation occurred. A line matching the maximum solubilities of aries within error subdivides the domains of solubility and precipitation.

Duel solute effect is a consequence of Gibbs-Duhem relation for a binary mixture within the COSMOSAC-LANL model

$$x_1 \mathrm{dln}\gamma_1 + x_2 \mathrm{dln}\gamma_2 = 0$$

Phys. Chem. Chem. Phys., Under Review, 2019

A. A. Shinkle, Univ. of Michigan, 2013; Journal of Power Sources 248 (2014)

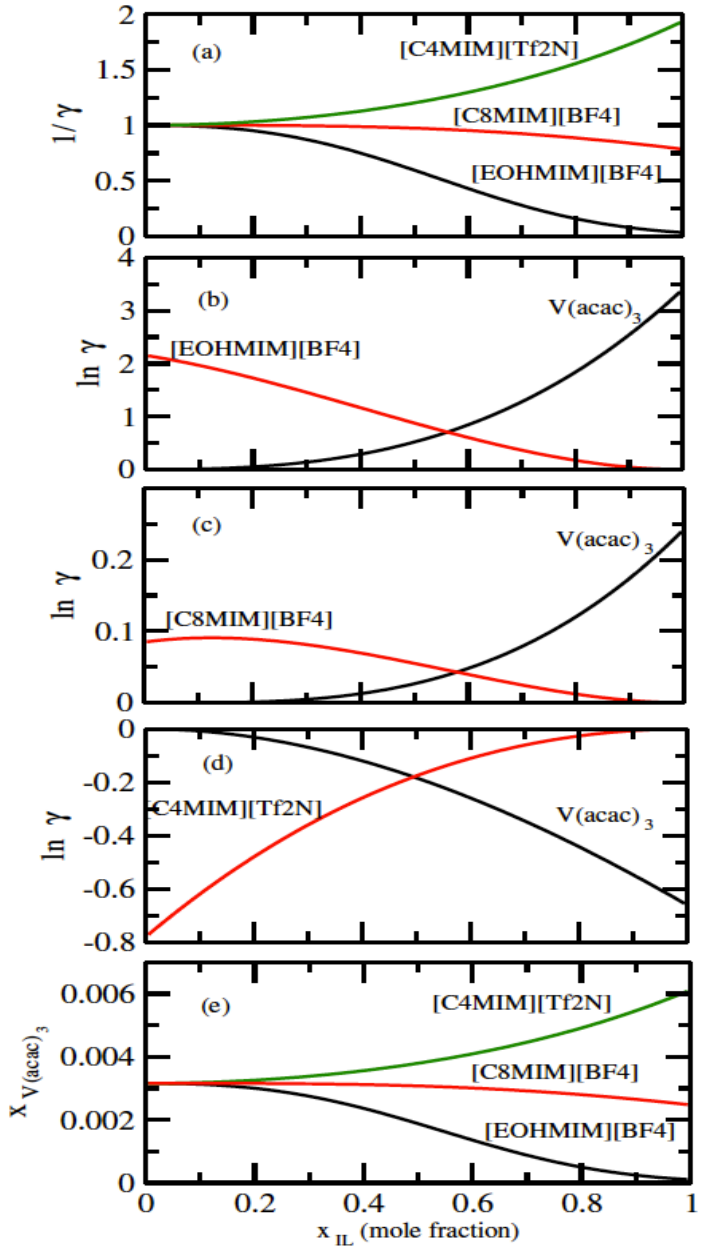

Figure 15: (a) The solubility has been shown as a function of $1/\gamma$. The Gibbs-Duhem relationships have been shown for (b) [EOHMIM][BF4], (c) [C8MIM][BF4] and (d) [C4MIM][Tf2N], respectively. (e) The calculated phase diagrams have been shown for all three ionic liquids.

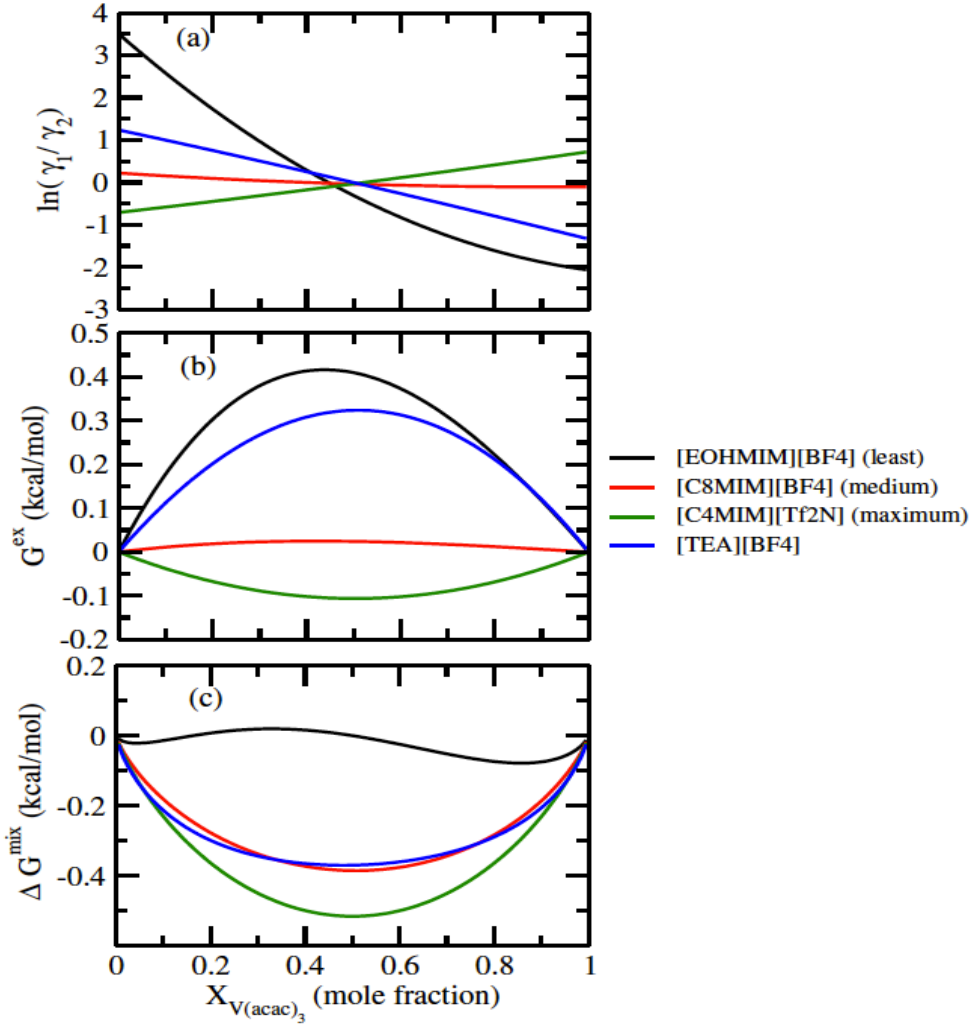

Figure 12: (a) $\ln\gamma_1/\gamma_2$, in fig (b) G^{ex} and, in fig (c) ΔG^{mix} have been shown as a function of solute mole fraction at 297 K.

Phys. Chem. Chem. Phys., Under Review, 2019

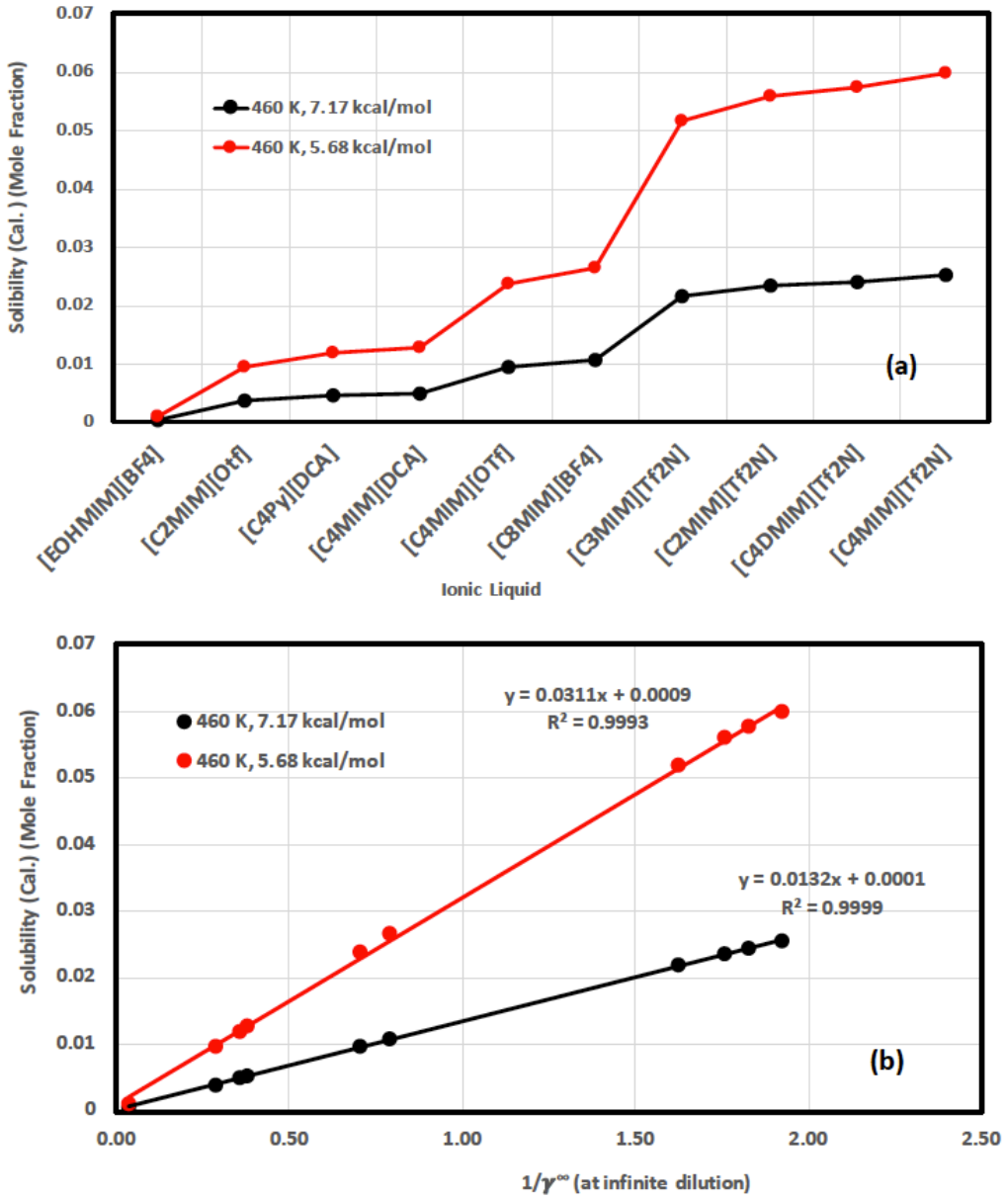

Figure 11: In Fig.(a) solubility of $V(acac)_3$ in 10 ionic liquids and in fig.(b) the solubility of $V(acac)_3$ in 10 ionic liquids is correlated with the activity coefficient at infinite dilution of the metal complex in ionic liquids for two different heat of fusions of $V(acac)_3$: ΔH_f = 7.17 kcal/mol (black) and ΔH_f = 5.68 kcal/mol (red).

From our theoretical calculations, we found that the solubility of these metal complexes will increase with increasing size of cation and anion of an ionic liquid. For all solubility calculations for $V(acac)_3$, we used melting temperature 460 K[48,49] and heat of fusion values 5.68 kcal/mol[49] and 7.17 kcal/mol[48] for Eq. 14. In the case of ideal solvation γ_{mc} =1, the percentage error in solubility is 2.12% for heat of fusion 7.17 kcal/mol and 4.31% for heat of fusion 5.68 kcal/mol calculated using Eq. 14. We repeated similar calculations for $Cr(acac)_3$ in ionic liquids for different heat of fusions and melting temperatures already reported in the literature.[48–53] We found a similarity with the results already obtained

- The relation between metal complex solubility and activity coefficient is

$$\ln x_{mc} = -\ln \gamma_{mc}(T,x) + \frac{\Delta H^{f}_{mc}(T_m)}{RT_m}\left(1 - \frac{T_m}{T}\right)$$

Phys. Chem. Chem. Phys., Under Review, 2019

Metal complex solubility in Organic solvents

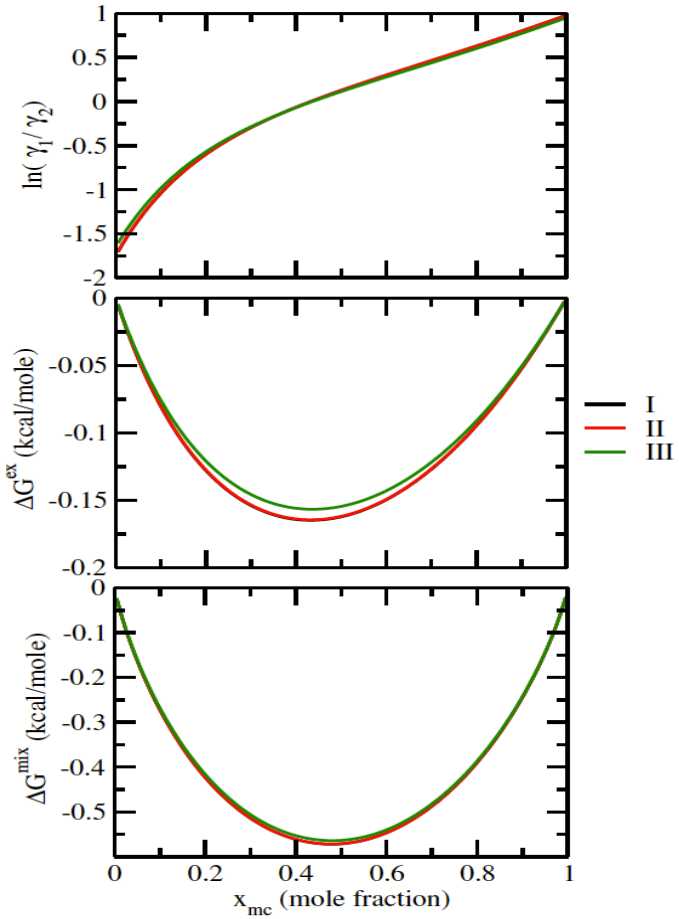

Figure 6: $\ln\gamma_1/\gamma_2$, in fig (b) G^{ex} and, in fig (c) G^{mix} have been shown as a function of solute mole fraction for the metal complexes with same ligands but different metal center. The γ_1 and γ_2 are the activity coefficient of the solute and solvent molecule, respectively. The solvent is Acetonitrile (ACN).

Solubility order

II>IV>V>VI

Thompson et. al., J. Mat. Chem. A, 2015, 2017

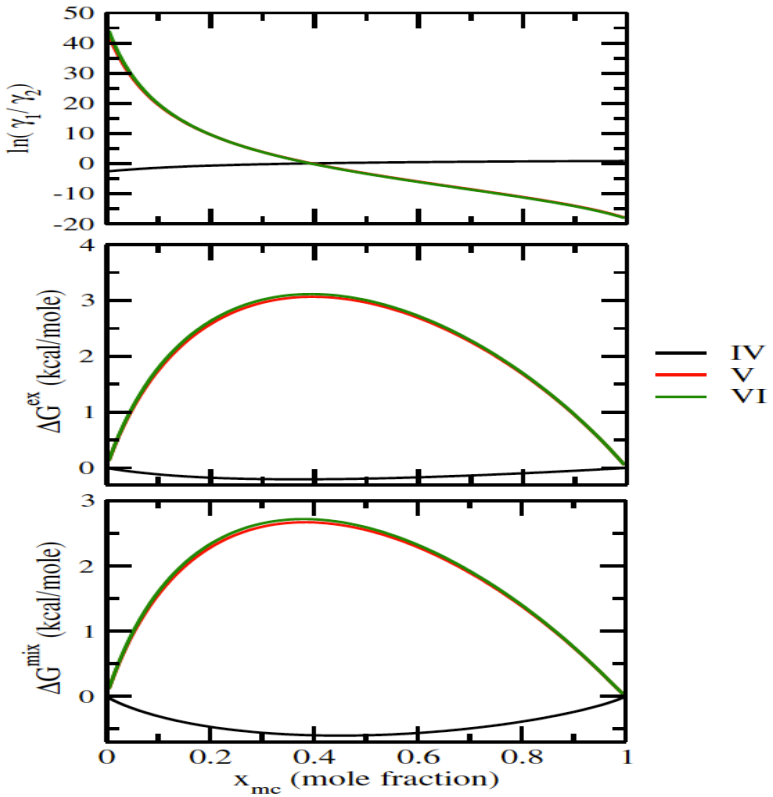

Figure 7: $\ln\gamma_1/\gamma_2$, in fig (b) G^{ex} and, in fig (c) G^{mix} have been shown as a function of solute mole fraction for the metal complexes with different ligands but same metal center. The γ_1 and γ_2 are the activity coefficient of the solute and solvent molecule, respectively. The solvent is Acetonitrile (ACN).

Metal complexes	COSMO Volume (Å^3)	COSMO Surface (Å^2)	Molar Mass (g/mol)	Exp. solubility (M) [1,46,47]
I	387.35	357.68	348.1	0.6[1] and 0.4[46]
II	383.47	357.32	358.01	0.65[46]
III	379.83	353.29	348.98	0.60[47]
IV	532.21	468.12	473.01	0.043[46]
V	672.93	581.58	597.05	8E10-4[46]
VI	697.31	818.12	721.01	6E10-5[46]

Table 2: The COSMO surface, volume, molar mass and experimental solubility of different metal complexes.

Phys. Chem. Chem. Phys., Under Review, 2019

Solubility of $V(acac)_3$ in different organic solvents

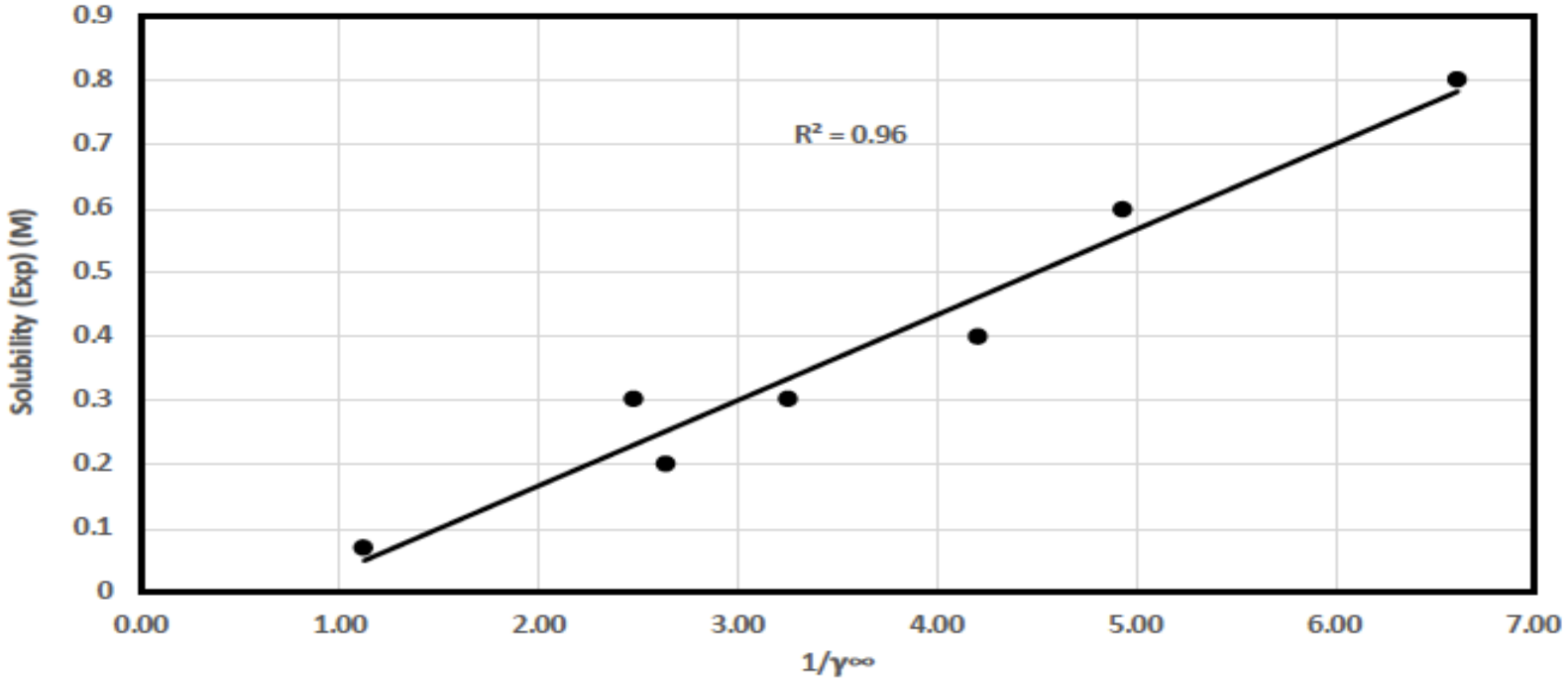

Solvents	$1/\gamma^{\infty}$	Exp. Sol. (M)
PC	1.12	0.07
GBL	3.25	0.3
DMPU	2.65	0.2
EA	2.48	**0.3**
AN	4.95	0.6
MA	4.22	0.4
13DO	6.62	0.8

A. Karmakar *et al.* (submitted); T. Herr *et al.*, Journal of Power Sources 265 (2014) 317-324.

Conclusions

- First principle based new activity coefficient models have been introduced
  - COSMOSAC-2013
  - COSMOSAC-LANL

  for whole range of concentration.

- The new thermodynamic model has been successfully applied to
  - Metal complex solubility in RTILs.
  - Metal complex solubility in organic solvents.

Other Applications

Solvent extraction in Hydrometallurgy in Nuclear Industry

"Historically, ***metal acetylacetonates*** are significant since they were among the earliest metal compounds which were recognized as what later became known as ***coordination compounds***. Additionally, they were significantly investigated during ***WWII*** as potentially useful in the ***separation of isotopes***, especially of ***uranium*** because of their unexpected volatility." -------- Evrim Arslan et al., 2016

Solvent extraction in Hydrometallurgy in Mining or Recycling

Applications in Pharmaceuticals ------- Mettalodrugs

"***Transition metal complexes*** offer two distinct advantages as ***DNA-binding agents***. First and foremost, transition metal centers are particularly attractive moieties for reversible recognition of nucleic acids research because they exhibit well-defined coordination geometries. Besides, they often show distinct ***electrochemical or photophysical properties***, thereby increasing the functionality of the binding agent. In fact, these smart features have fueled the complexes to be used in a broad spectrum of applications, from ***fluorescent markers to DNA footprinting agents, to electrochemical probes***."------ Natarajan Raman et al. 2016

Acknowledgement

- The research leading to this results has received funding from "Laboratory Directed Research and Development" program grant no. 20170046DR in Los Alamos National Laboratory, USA.

Thank You !